Estimation of Nitrogen Load from Septic Systems to Surface Water Bodies in the Indian River Lagoon (Main-South Canal drainage basin)

Manuscript Completed: August 2015

Prepared by

Mohammad Sayemuzzaman, and Ming Ye

Department of Scientific Computing, Florida State University, Tallahassee, FL 32306

Rick Hicks, FDEP Contract Manager

Prepared for

Florida Department of Environmental Protection

Tallahassee, FL

THIS PAGE INTENTIONALLY LEFT BLANK

EXECUTIVE SUMMARY

The ArcGIS-based Nitrate Load Estimation Toolkit (ArcNLET), which was developed for the Florida Department of Environmental Protection (FDEP) by the Florida State University (FSU), was used in this study to the drainage basins of Main Canal(MC) and South Canal(SC) of Indian River County (IRC). The load estimates can be used to calculate credit for septic tank phase out projects in support of the on-going Basin Management Action Plan (BMAP).While ArcNLET is based on a simplified model of groundwater flow and nitrogen transport, the model considers heterogeneous hydraulic conductivity and porosity as well as spatial variability of septic system locations, surface water bodies, and distances between septic systems and surface water bodies. ArcNLET also considers key mechanisms controlling nitrogen transport, including advection, dispersion, and denitrification. After preparing model input files (e.g., raster file of hydraulic conductivity) in the ArcGIS format, setting up an ArcNLET model run is easy through a graphic user interface. The modeling results are readily available for post-processing and visualization within ArcGIS. The modeling results include Darcy velocity, groundwater flow paths from septic systems to surface water bodies, spatial distribution of nitrogen plumes, and nitrogen load estimates to individual surface water bodies; these results can be used directly for environmental management and regulation of nitrogen pollution.

The ArcNLET flow and transport models of this study were established using the data downloaded from public-domain websites and provided by colleagues from FDEP. Site-specific data of DEM, waterbodies, septic locations, hydraulic conductivity, and porosity were used in the ArcNLET modeling. Literature-based smoothing factor for flow modeling and transport parameters, including longitudinal dispersivity (α_L), transverse horizontal dispersivity (α_{TH}), decay coefficient (k), inflow mass to groundwater (M_{in}), and source plane concentration (C_0) were used in the transport modeling. These parameter values are listed in Table ES-1. The calibrated ArcNLET models are used to simulate nitrogen plumes and estimate nitrogen load from the removed septic systems to surface water bodies.

Table ES-0-1. Calibrated values of ArcNLET only model parameters for this modeling. Calibration of flow and transport parameters for the IRL (South-Main canal of IRC).

Parameter	IRL (South-Main canal of IRC)
Smoothing factor	65
C_0 (mg/L)	40
α_L (m)	1
α_{TH} (m)	0.1
k (d^{-1})	0.00055

The calibrated ArcNLET models are used to simulate nitrogen plumes and estimate nitrogen load from the removed septic systems to surface water bodies. The simulated nitrogen plumes and load estimates exhibit substantial spatial variability, which manifests the importance of considering spatial variability in the load estimation. In the IRC-SM modeling, the canals are

distributed over the entire modeling area, thus effective management of nitrogen pollution should be conducted over the entire modeling area.

Table ES-0-2: Loading summary (using ArcNLET alone). Main and South canal drainage basins contributed load, and load per septic system.

	Area (acre)	No of Septic tanks	lbs/yr	lbs/yr/septicTank
Main canal	24666	5346	4548.73	0.85
South Canal	15122	7395	8922.25	1.21
Total	39788	**12741**	**13470.98**	**1.06**

Table ES-0-3: Loading summary (using VZMOD+ArcNLET)

	Total output Load (g/d)	**Total output Load (lbs/yr)**	Total Input Mass (g/d)	Load Reduction (%)	**Load/ Septic Tank (g/d)**	**Load/Septic Tank (lbs/yr)**
NH4	**93.73**	**75.44**	2003.13	95.32	**0.01**	**0.01**
NO3	**17505.70**	**14089.03**	248973.13	92.97	**1.37**	**1.11**
Total	**17599.43**	**14164.47**	250976.25	92.99	**1.38**	**1.12**

CONTENTS

LIST OF FIGURES

LIST OF TABLES

1. INTRODUCTION

This study is aimed at supporting management of coastal nitrogen pollution, which is considered as the most prevalent and challenging pollution problem currently facing U.S. coastal waters (National Research Council, 2000). The pollution has resulted in serious environmental, ecological, economical, and human health problems, such as groundwater contamination, methemoglobinemia (also known as blue baby syndrome), eutrophication, fish kills, harmful algal growth, and some shellfish poisoning (Walters, 1983; National Research Council, 2000; Howarth, 2008). In the continental United States, moderate to severe degradation of water quality due to nitrogen and phosphorus pollution has been reported in more than 60 percent of coastal rivers and bays (Howarth et al., 2000). Among the various nitrogen sources (e.g., atmospheric deposition, fertilizer use, and wastewater discharge), an important source of nitrogen in the environment, especially in highly populated coastal areas, is due to wastewater treatment using onsite sewage treatment and disposal systems (OSTDS) (a.k.a., septic systems). According to U.S. Environmental Protection Agency (USEPA, 2003), approximately 25% of the homes and 33% of new developments in the United States utilize septic systems; in the state of Florida, nearly one-third of households use septic systems (Ursin and Roeder 2008). In the Chesapeake Bay watershed that includes multiple states, 25% of the population utilizes septic systems (Maizel et al., 1997). Valiela and Costa (1988) showed that, in Buttermilk Bay, MA, 40% of nitrogen and phosphorous entering watershed was from septic systems and 80% of the nitrogen was transported through groundwater. In the Waquoit Bay, MA, 48% nitrogen load was from septic systems (Valiela et al., 1997). In the study of Kroeger et al. (2006) at Cape Cod, wastewater from septic systems is considered as the principal source of nitrogen entering estuaries from urbanized or suburbanized watersheds. For the Chesapeake Bay watershed of larger scale, a recent study (USEPA, 2013) indicates that septic systems contribute approximated 8.3 million pounds to the Bay, about 5% of the total nitrogen load. While this is not the largest source of nitrogen pollution to the Bay, it is important to reduce the load from septic systems in the effort to improve water quality. Given the trends in population growth, nitrogen loads from septic systems are expected to increase. Therefore, sustainable decision-making and management of nitrogen pollution due to septic systems are urgently needed.

The site of interest to this study is the South-Main Canal drainage basin and City of Sebastian (Figure 1-1) located in Indian River County in southeast Florida. It is a major tributary to the Southern Indian River Lagoon, where the ecological and biological integrity has deteriorated in the last several decades due to the decline in water quality caused in part by nitrogen pollution (Sigua et al., 2000). Nitrogen load from septic systems is an important reason to nitrogen pollution. A study of Sigua and Tweedale (2003) showed that, at the Indian River Lagoon, the load from groundwater seepage is 84,920 kg/year, about 8% to the overall nitrogen loading, the second largest source after the agricultural/urban runoff which contributes 79% of the load. In the groundwater load, a large portion is expected to be from septic systems, especially in areas with high population density such as the South-Main Canal drainage basin.

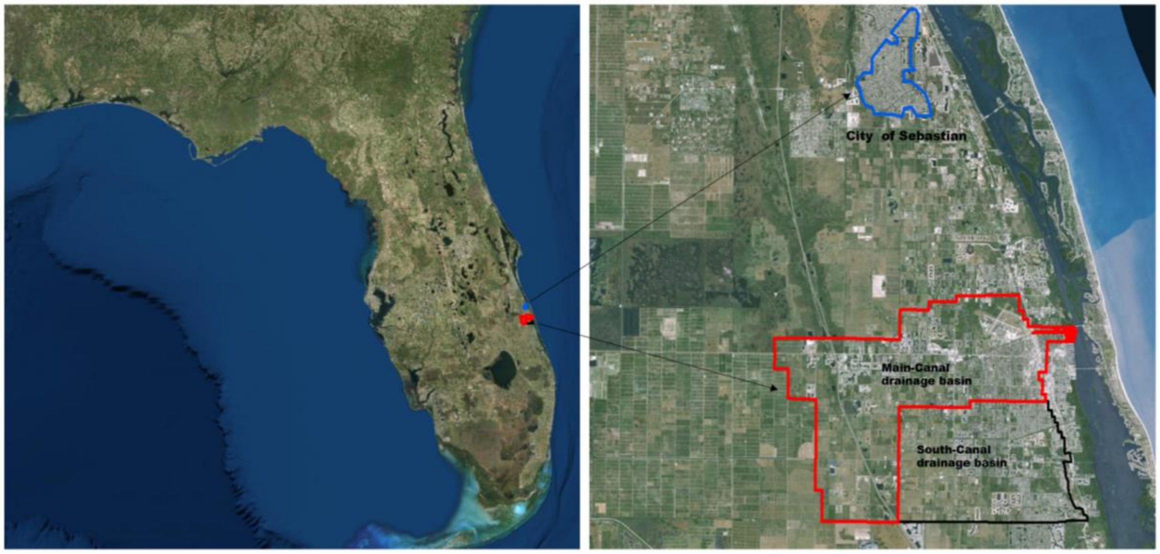

Figure 1-1. Location of Main-South Canal drainage basin (red-black thick lines) and City of Sebastian (blue thick lines) in Florida, USA.

The Florida Department of Environmental Protection has adopted Total Maximum Daily Loads (TMDL) to reduce the watershed nutrient inputs to the Indian River Lagoon (IRL). In support of the TMDL implementation, the Basin Management Action Plan (BMAP, 2013) has been developed. The BMAP includes various management means, and one of them is to convert septic into sewage. However, nitrogen load reduction due to the septic system removal is still unknown. Quantifying the reduction is important for planning and controlling of wastewater nitrogen loading, as well as to nitrogen trading and offset program described in U.S. EPA (2013), which can help minimize overall cost of TMDL implementation.

There have been no well-accepted techniques to estimate nitrogen loads from septic systems (removed or functioning). In certain methods, load estimates are given from interpolation and extrapolation of field measurements, such as in the studies of Reay (2004) at Chesapeake Bay and Sigua and Tweedale (2004) at Indian River Lagoon. While modeling approaches are more popular and practical, the models of load estimation range from simple arithmetic calculation based on empirical rules to sophisticated evaluation based on state-of-the-art understanding of physical, chemical, and biological processes and their interactions involved in nitrogen transport. In the Nitrogen Load Model (NLM) of Valiela et al. (1997, 2000), the load from septic systems is evaluated in a simple way as: nitrogen released per person per year × people/house × number of houses × 60% not lost in septic tanks and leaching fields × 66% not lost in plumes × 65% not lost in aquifer. The coefficients were derived from literature, limited filed data, and/or best engineering judgment. This NLM-kind modeling method has been used widely. For example, Vadeboncoeur et al. (2010), Giordano et al. (2011), and Kinney and Valiela (2011) estimated nitrogen load to Narragansett Bay, Virginia Lagoon, and Great South Bay, respectively, by multiplying literature-derived load coefficients to various nitrogen sources. More such models can be found in the NLOAD software developed by Bowen et al. (2007), an interactive, web-based modeling tool for nitrogen management in estuaries While the NLM model yields satisfactory results in comparison with field measurements (Valiela et al., 2000), justification of using the coefficients for new sites remains challenging, especially when there is no measurement of nitrogen loads to evaluate accuracy of the coefficients. In addition, the coefficients do not explicitly consider spatial variability of nitrogen concentrations and cannot reflect heterogeneity of hydrogeological properties (e.g., hydraulic conductivity) and distance of septic systems to surface water bodies. The variability cannot be ignored. For example, Sigua and Tweedale (2004) reported that the nitrogen concentration in the central Indian River Lagoon can be twice as large as that in the northern Lagoon. As a result, the estimated nitrogen loads using the NLM-type methods may not be sufficient for providing site-specific information for effective management of nitrogen pollution and implementation of TMDL.

In the wide spectrum of nitrate models, one extreme is to consider, to the extent possible, all biohydrogeochemical processes involved in nitrate/nitrogen fate and transport. For example, Maggi et al. (2008) developed a numerical code, TOUGHREACT-N, one of the most sophisticated code to date, for simulating coupled processes of advective and diffusive nutrient transport, multiple microbial biomass dynamics, and equilibrium and kinetic chemical reactions in soil and groundwater. While this model has the potential of being applied for coastal areas, the applications have not been reported in literature. Instead, simplified models have been used. Meile et al. (2010) and Porubsky et al. (2011) developed a two-dimensional model that numerically solves the advection-dispersion equation coupled with the reaction network encompassing reactions of sorption-desorption, nitrification, denitrification, and dissimilatory nitrate reduction to ammonium. A similar simplified model can be found in Spiteri et al. (2008) with focus on modeling biogeochemical processes for simulating nutrients in submarine groundwater discharge. These complex models can handle spatial variability of hydrogeologic properties and distance of septic systems to surface water bodies, and may yield results that can potentially agree well with field observations. However their complexity may be a hurdle for general users to set up the models; a trained professional is always required to operate the models and interpret modeling results for decision-makers of environmental management. In addition, to utilize sophisticated functions of the models, a large amount of model input and calibration data as well as long execution time may be needed, which may not be available or affordable in practice. For many management projects of nitrate transport modeling and load estimation, including those related to environmental regulation such as total maximum daily load (TMDL), it may not be practical to use the complex models. Therefore, alternative modeling methods are needed.

Models based on Geographic Information System (GIS) have gained popularity in environmental modeling (National Research Council, 2010). GIS-based screening models are one of the six primary types of models to facilitate modeling assessment and decision-making associated with pollutants from septic systems (McCray et al., 2009). GIS is an efficient tool to integrate regional/local spatial characteristics (e.g., digital hydrologic and topographic data) of a system. GIS-based models here are not GIS tools simply for preparing model input files and post-processing output files of other modeling programs. Instead, the GIS-based models provide a modeling environment for simulating quantities of interest and for analyzing and visualizing modeling results by non-technical citizens. A number of GIS-based modeling software have been developed, including PRO-GRADE (Lin et al. 2009) and uWATER-PA (Yang and Lin 2011; Rios et al., 2011a) for groundwater problems, TNT2 (Beaujouan et al. 2002) and GWLF (Romshoo and Muslim, 2011) for nitrogen transport and load estimation, and WARMF (Herr et al. 2001) for calculation of TMDLs for most conventional pollutants at the watershed scale. The GIS-based models and software always have a simple conceptual model and use computationally inexpensive methods that can be implemented within GIS. For example, Becker and Jiang (2007) developed a GIS-based groundwater contaminant transport model using the analytic element method. Focusing on nitrate pollution from agricultural sources, Schilling and Wolter (2007) developed a GIS-based model to estimate groundwater travel time using DEM data. The GIS-based models can be viewed as a compromise between the rule-based models (e.g., NLM) and the sophisticated numerical models (e.g. TOUGHREACT-N), with the attractive features of incorporating site-specific information (e.g., DEM), considering spatial variability of hydrogeologic properties, and simulating hydrogeochemical processes involved in nitrogen transport. There are other reasons that render GIS-based models suitable to environmental management. For example, skills required for applying GIS-based models are widely available; the models are easy to set up and computationally efficient to execute; the modeling process is transparent; the modeling results are readily available to interpret and visualize within GIS; and the results are quantitative and can be used directly for environmental management and regulation.

The ArcGIS-Based Nitrate Load Estimation Toolkit (ArcNLET, Rios et al. 2013a; Wang et al., 2013) is used in this study to simulate nitrate transport in surficial aquifers due to septic systems and to estimate corresponding nitrate load to surface water bodies. ArcNLET considers advection, hydrodynamic dispersion, and denitrification processes involved in nitrate transport. It also incorporates heterogeneous hydraulic parameters that vary by raster elements and considers spatial variation of locations and loads from individual septic systems. In addition, as shown in Wang et al. (2013), ArcNLET is able to simulate field observations at specific sites. However, similar to other GIS-based models, ArcNLET relies on a simple conceptual model involving a number of assumptions and simplifications, and uses an analytical equation to describe nitrogen transport. Therefore, ArcNLET should be used as a screening model to provide quick estimates, especially when field data are insufficient to calibrate parameters that are needed to simulate groundwater flow and nitrogen transport.

ArcNLET is used in this study to simulate nitrate load from removed septic systems at two sites in the City of Sebastian and Main-South Canal drainage area to surface water bodies. The load estimates can be used directly to support the on-going TMDL implementation in the coastal estuary. ArcNLET is used to simulate the loads from the individual sites. For the sites (e.g., the Main-South Canal drainage area) where monitoring data of hydraulic head and nitrogen concentration are available, model calibration is conducted in the trial-and-error manner to estimate values of model parameters such as dispersivity and denitrification coefficient. The simulated results are evaluated by comparing them with literature data and those obtained using other methods. The results are also discussed in the context of Basin Management Action Plan (BMAP) to evaluate the relative contribution of the septic-related load to the total nitrogen load; a scenario analysis is conducted to estimate the amount of nitrogen load reduction if functioning septic systems are converted to sewer.

Measured nitrogen concentrations in the Main-South Canal drainage basin area is different from those in Jacksonville, FL., in that concentrations of ammonimum and TKN are higher than those of nitrate, which may be attributed to incomplete nitrification process in the vadose zone. This poses a challenge to ArcNLET modeling, since it is developed for nitrate transport modeling. While developing a new ArcNLET version to simulate ammonium transport is warranted in a future study, it is not attempted in this study. Instead, the calibration target is the concentration of total nitrogen or dissolved inorganic nitrogen (DIN) (including ammonium, nitrite, and nitrate), depending on availability of ammonium or TKN concentrations. This is tantamount to assuming that the transport mechanisms of ammonimum and/or organic nitrogen are the same as those of nitrate, which diregards the processes of nitrification, adsorption, and other reactions. Their effects on accuracy of the load estimates have not been investated but are not expected to be significant.

The estimates of nitrogen loading are inherently uncertain, because of the lack of information and data to fully characterize and simulate hydrology and hydrogeology of the modeling sites and the biogeochemical processes involved in nitrogen transport. Valiela et al. (1997) estimated that the uncertainty of model simulated load is approximately 37-38% due to uncertainty in the coefficients used in the NLM modeling. In this study, there is calibration of flow and transport parameters (e.g., hydraulic head, dispersivities, and denitrification parameters). Although model calibration is conducted to estimate the parameter values, the monitoring data is too scarce to yield parameter estimates with small uncertainty.

In the remainder of this report, the conceptual model groundwater flow and nitrogen transport used in ArcNLET and its computational implementation are briefly described in Section 2. Section 3 presents the hydrologic and hydrogeologic conditions of the modeling areas as well as the historical monitoring data compiled in this study for model calibration. The results of model calibration and load estimation are given in Section 4. The summary and conclusions of this study are discussed in Section 5.

2. SIMPLIFIED CONCEPTUAL AND MATHEMATICAL MODEL OF ARCNLET

ArcNLET is based on a simplified conceptual model of groundwater flow and nitrate transport. The model has three sub-models: groundwater flow model, nitrate transport model, and nitrate load estimation model. The three submodels are briefly described here; more details of them can be found in Rios (2010) and Rios et al. (2013a).

The groundwater flow model of ArcNLET is simplified by assuming that the water table is a subdued replica of the topography in the surficial aquifer. According to Haitjema and Mitchell-Bruker (2005), the assumption is valid if

$$\frac{RL^2}{mKHd} > 1, \tag{1}$$

where R [m/day] is recharge, L [m] is average distance between surface waters, m is a dimensionless factor accounting for the aquifer geometry, and is between 8 and 16 for aquifers that are strip-like or circular in shape, K [m/day] is hydraulic conductivity, H [m] is average aquifer thickness, and d [m] is the maximum distance between the average water level in surface water bodies and the elevation of the terrain. The criterion, as a rule of thumb, can be met in shallow aquifers in flat or gently rolling terrain. Based on the assumption, the shape of water table can be obtained by smoothing land surface topography given by DEM of the study area. In ArcNLET, the smoothing is accomplished using moving-window average via a 7 × 7 averaging window. The smoothing process needs to be repeated for multiple times, depending on discrepancy between the shapes of topography and water table. The number of the smoothing process, called smoothing factor, is specified by ArcNLET users as an input parameter of ArcNLET. This parameter needs to be calibrated against measured hydraulic heads in the study area, as explained in detail in Section 4.

With the assumption that smoothed DEM has the same shape (not the same elevation) of water table, hydraulic gradients can be estimated from the smoothed DEM. Subsequently, groundwater seepage velocity, v, can be obtained by applying Darcy's Law

$$\begin{aligned} v_x &= -\frac{K}{\phi}\frac{\partial h}{\partial x} \approx -\frac{K}{\phi}\frac{\partial z}{\partial x} \\ v_y &= -\frac{K}{\phi}\frac{\partial h}{\partial y} \approx -\frac{K}{\phi}\frac{\partial z}{\partial y} \end{aligned}, \tag{2}$$

where K is hydraulic conductivity [LT^{-1}], ϕ is porosity, h is hydraulic head, and hydraulic gradient ($\partial h/\partial x$ and $\partial h/\partial y$) is approximated by the gradient of the smoothed topography ($\partial z/\partial x$ and $\partial z/\partial y$). Implementing the groundwater flow model in the GIS environment yields the magnitude and direction of the flow velocity for every discrete cell of the modeling domain, which are used to estimate flow paths originating from individual septic systems and ending in surface water bodies. The calculation considers spatial variability of hydraulic conductivity, porosity, hydraulic head, and septic system locations. Because hydraulic gradients and water bodies are not hydraulically linked in the model, ArcNLET users need to evaluate whether the resulting shape of the water table is consistent with the drainage network associated the water bodies. The values of hydraulic conductivity and conductivity can be obtained from field measurements, literature data, and/or by calibration against measurements of hydraulic head and groundwater velocity.

Additional assumptions and approximations of the flow model are made as follows: (1) the Dupuit-Forchheimer assumption is used so that the vertical flow can be ignored and only two-dimensional (2-D) isotropic horizontal flow is simulated; (2) the steady-state flow condition is assumed, since this software is used for the purpose of long-term environmental planning; (3) the surficial aquifer does not include karsts or conduits so that Darcy's Law can be used; (4) mounding on water table due to recharge from septic systems and rainfall is not explicitly considered (but assumed to be reflected by the steady-state water table); (5) the flow field is obtained from the water table without explicit consideration of a water balance; (6) groundwater recharge from the estuary is disregarded. While these assumptions may not be ideal, especially the assumption of steady-state, they are needed to make model complexity compatible with available data and information and to make the model run efficient in the GIS modeling environment.

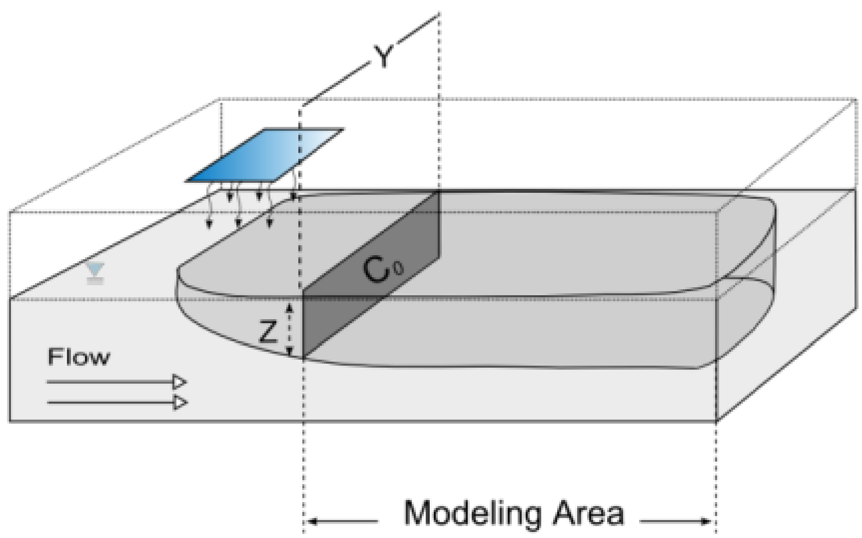

Figure 2-1. Conceptual model of nitrate transport in groundwater adapted from Aziz et al. (2000). The unsaturated zone is bounded by the rectangular box delineated by the dotted lines; the groundwater zone is bounded by the box delineated by the solid lines

Figure 2-1 shows the conceptual model of nitrate transport in ArcNLET, which is similar to that of BIOSCREEN (Newell et al. 1996) and BIOCHLOR (Aziz et al. 2000) developed by the U.S. EPA. In the conceptual model, nitrate enters the groundwater zone with a uniform and steady flow in the direction indicated. The Y−Z plane in Figure 2-1 is considered as a source plane (with a constant concentration C_0 [ML^{-3}]) through which nitrate enters the groundwater system.

This portion of writing describes the conceptual and mathematical models of nitrogen fate and transport in the vadose zone and groundwater. The conceptual and mathematical models of vadose zone processes in the new ArcNLET code are those of VZMOD described previously by Wang et al. (2012, 2013b). Briefly, VZMOD calculates saturation and concentration profiles between each drain field and the water table for steady-state, one-dimensional vertical reactive transport with constant incoming water, ammonium and nitrate fluxes. VZMOD is seamlessly integrated with ArcNLET in the following ways. First, the water table estimated from the ArcNLET groundwater modeling is used as the bottom boundary of the vadose zone modeling of VZMOD. The distance between drain field infiltrative surface and water table is estimated based on the digital elevation model (DEM) of the ground surface and an estimate for the water table. VZMOD assumes a constant depth of drain field infiltrative surfaces below ground surface, 18 inches in this study (Wang et al., 2012). The water table elevation is estimated by subtracting a constant from the smoothed DEM given by ArcNLET as discussed below. This constant is the intercept of a linear regression between observed water table at monitoring wells and their corresponding smoothed DEM elevation. Examples of determining the constant can be found in Wang et al. (2012, 2013a, 2013b). When the estimated distance between the drain field and water table is negative near surface water bodies, VZMOD assumes a small distance (e.g., 0.1 cm), which corresponds to negligible nitrification. This distance could be modified to account for modern onsite systems, such as mound systems, which maintain a water table separation. Second, the ammonium and nitrate concentrations, but not necessarily the mass flux, given by VZMOD at the water table, are used as the inputs to the modeling of ammonium and nitrate fate and transport in groundwater in the new version of ArcNLET.

Now the model estimates reactive advective-dispersive transport along each flow path at the average velocity and calculates the load to the surface water body.

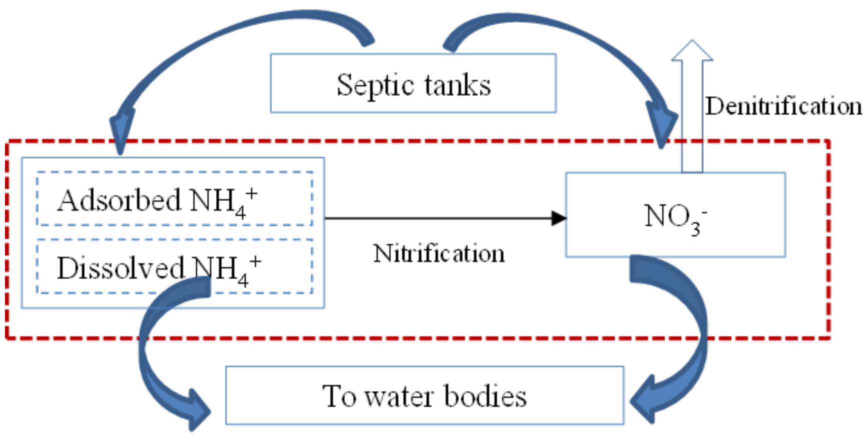

Fig. 1. Conceptual model of ammonium and nitrate transformation in groundwater used for the new ArcNLET code. The red box indicates the groundwater system.

The two-dimensional reactive transport of ammonium and nitrate is assumed to be steady state, and the governing equations are as follows:

$$0 = D_x \frac{\partial^2 c_{NH_4^+}}{\partial x^2} + D_y \frac{\partial^2 c_{NH_4^+}}{\partial y^2} - v \frac{\partial c_{NH_4^+}}{\partial x} - k_{nit}(1+\frac{\rho k_d}{\theta})c_{NH_4^+} \quad (3)$$

$$0 = D_x \frac{\partial^2 c_{NO_3^-}}{\partial x^2} + D_y \frac{\partial^2 c_{NO_3^-}}{\partial y^2} - v \frac{\partial c_{NO_3^-}}{\partial x} + k_{nit}(1+\frac{\rho k_d}{\theta})c_{NH_4^+} - k_{deni} c_{NO_3^-} \quad (4)$$

where D_x and D_y $[L^2T^{-1}]$ are the dispersivity coefficients in the longitudinal (x) and horizontal transverse (y) directions, respectively;   and $[ML^{-3}]$ are the concentrations of ammonium and nitrate, respectively; v $[LT^{-1}]$ is linear groundwater velocity in the longitudinal direction; ρ $[ML^{-3}]$ is bulk density, k_d $[L^3M^{-1}]$ is linear adsorption coefficient of ammonium; k_{nit} and k_{denit} $[T^{-1}]$ are the first-order decay coefficients of nitrification and denitrification, respectively; and θ [-] is effective porosity. Equations (3) and (4) are based on the principle of mass conservation, and can be derived by following the standard procedure given in textbooks such as that of Zheng and Bennett (2002). The last term at the right hand side of equation (3) is the same as the second to the last term at the right hand side of equation (4) and considers nitrification of dissolved and adsorbed ammonium with first-order kinetics. The last term at the right hand side of Equation (4) describes the denitrification of nitrate with first-order kinetics. The boundary conditions for the ammonium and nitrate transport assume a vertical source plane underneath the drain field and are as follows:

$$c_{NH_4^+}(0,y) = \begin{cases} c_{NH_4^+,0} & -\frac{Y}{2} < y < \frac{Y}{2} \\ 0 & \text{elsewhere} \end{cases}; \quad \lim_{x\to\infty} \frac{\partial c_{NH_4^+}(x,y)}{\partial x} = 0; \quad \lim_{y\to\pm\infty} \frac{\partial c_{NH_4^+}(x,y)}{\partial y} = 0 \qquad (5)$$

$$c_{NO_3^-}(0,y) = \begin{cases} c_{NO_3^-,0} & -\frac{Y}{2} < y < \frac{Y}{2} \\ 0 & \text{elsewhere} \end{cases}; \quad \lim_{x\to\infty} \frac{\partial c_{NO_3^-}(x,y,t)}{\partial x} = 0; \quad \lim_{y\to\pm\infty} \frac{\partial c_{NO_3^-}(x,y,t)}{\partial y} = 0 \qquad (6)$$

where Y is the width of a source plane introduced for estimating the mass of ammonium and nitrate. By adopting the pseudo three-dimensional model used in EPA BIOCHLOR model (Aziz et al., 2000), it is assumed that contaminants from a septic drain field form a vertically oriented plane with the size of Y in the width and Z in the height. The Y-Z plane has a constant concentration,   for ammonium and   for nitrate, and the contaminants enter the groundwater aquifer by advection and dispersion. The origin of the coordinate system is located at the center of the Y-Z plane with the positive x and y directions rightward and upward, respectively. While the source plane concentrations can be evaluated by using VZMOD, if the simulated concentrations of VZMOD are zero, a small value of 10-4 mg/L is assigned to   and   to avoid numerical instability. This small value does not affect the ultimate load estimation.

Analytical solutions of equations (3) and (4) used in the new ArcNLET code allow incorporation of ammonia while requiring only slight modifications to the algorithms described by Rios et al. (2013). The analytical solutions are obtained by using the method of Sun et al. (1999) that transforms the two coupled equations into two independent equations. This is done by defining the auxiliary variables,

$$a_{NH_4^+} = c_{NH_4^+} \qquad (7)$$

$$a_{NO_3^-} = c_{NO_3^-} + \frac{k_{nit}(1+\rho k_d/\theta)}{k_{nit}(1+\rho k_d/\theta) - k_{deni}} c_{NH_4^+} \qquad (8)$$

With the auxiliary variables, equation (3) does not change, except that is replaced by; equation (4) is transformed to

$$0 = D_x \frac{\partial^2 a_{NO_3^-}}{\partial x^2} + D_y \frac{\partial^2 a_{NO_3^-}}{\partial y^2} - v \frac{\partial a_{NO_3^-}}{\partial x} - k_{deni} a_{NO_3^-} \qquad (9)$$

Therefore, the two transformed equations have the same form below

$$D_x \frac{\partial^2 a_i}{\partial x^2} + D_y \frac{\partial^2 a_i}{\partial y^2} - v \frac{\partial a_i}{\partial x} - k_i a_i = 0 \quad (i = NH_4^+, NO_3^-)$$

$$k_i = \begin{cases} k_{nit}(1 + \frac{\rho k_d}{\theta}) & i = NH_4^+ \\ k_{deni} & i = NO_3^- \end{cases} \qquad (10)$$

For equation (10), the analytical solution of Domenico (1987) is used, and its simplification for the two-dimensional, steady-state condition is (Rios et al., 2013)

$$a(x, y) = \frac{a_0}{2} \times F_1(x) \times F_2(y, x) \qquad (11)$$

$$F_1(x) = \exp\left[\frac{x}{2\alpha_x} \left(1 - \sqrt{1 + \frac{4k\alpha_x}{v}} \right) \right] \qquad (12)$$

$$F_2(y, x) = erf\left(\frac{y + Y/2}{2\sqrt{\alpha_y x}} \right) - erf\left(\frac{y - Y/2}{2\sqrt{\alpha_y x}} \right) \qquad (13)$$

where erf is the error function, and α_x and α_y [L] are longitudinal and horizontal transverse dispersivity, respectively. After solving equation (10) for the auxiliary variables a_i, the concentrations of ammonium and nitrate are obtained by back-transforming equations (7) and (8) as follows,

$$c_{NH_4^+} = a_{NH_4^+} \qquad (14)$$

$$c_{NO_3^-} = a_{NO_3^-} - \frac{k_{nit}(1 + \rho k_d / \theta)}{k_{nit}(1 + \rho k_d / \theta) - k_{deni}} a_{NH_4^+} \qquad (15)$$

Using the method of Sun et al. (1999) enables using the analytical solution of the same form for a_i, and thus saves computational time and reducing complexity of the software development. In the ArcNLET numerical implementation of the analytical solutions, the modeling domain is discretized into a grid of uniform cells with the size of $\Delta x \times \Delta y$, and for a given plume the concentrations are evaluated for each cell. This approach of raster discretization allows capturing the effect of overlapping plumes (Rios et al., 2013).

Finally, the loadings of ammonium and nitrate are estimated using a mass-balance approach for the final rasterized concentration field. The nitrogen mass entering the water bodies equals to the difference between nitrogen entering groundwater and nitrogen removal during the groundwater transport. Specifically speaking, the ammonium and nitrate loadings for each plume are estimated via

$$M_{NH_4^+,out} = M_{NH_4^+,in} - M_{nit} \tag{16}$$

$$M_{NO_3^-,out} = M_{NO_3^-,in} + M_{nit} - M_{deni} \tag{17}$$

where and [MT^{-1}] are the mass outflow rate (i.e., the loadings) of ammonium and nitrate, respectively, to surface water bodies; and [MT^{-1}] are the mass inflow rate of ammonium and nitrate, respectively, from septic systems to groundwater; M_{nit} [MT^{-1}] is the ammonium mass removal rate due to nitrification, and M_{denit} [MT^{-1}] is the nitrate mass removal rate due to denitrification. The mass removal rates caused by nitrification and denitrification are calculated as

$$M_{nit} = \sum_j k_{nit}(1+\rho k_d/\theta) \times c_{NH_4^+,j} \times V_j \times \theta \tag{18}$$

$$M_{deni} = \sum_j k_{deni} \times c_{NO_3^-,j} \times V_j \times \theta \tag{19}$$

where V_j [L^3] is the volume of the j-th cell of the ammonium and nitrate plumes. The volume is calculated as Δx × Δy × Z, where Z [L] is the height of source plane, and Δx and Δy [L] are the cell sizes in the x and y directions determined by the ArcNLET users and input through ArcNLET user interface discussed in Section 3. The values of Z used in the calculation can be estimated in the two ways discussed below.

By considering advective and dispersive mass flux, the equation for estimating inflow mass rates were derived in Appendix A, and they are

$$M_{NH_4^+,in} = c_{NH_4^+,0} YZ\theta v \left(\frac{1+\sqrt{1+\frac{4k_{nit}(1+\rho k_d/\theta)\alpha_x}{v}}}{2} \right) \tag{20}$$

$$M_{NO_3^-,in} = a_{NO_3^-,0} YZ\theta v \left(\frac{1+\sqrt{1+\frac{4k_{deni}\alpha_x}{v}}}{2} \right) - \frac{k_{nit}(1+\rho k_d/\theta)}{k_{nit}(1+\rho k_d/\theta)-k_{deni}} \times M_{NH_4^+,in} \tag{21}$$

where $a_{NO_3^-,0}$ is the auxiliary variable of $c_{NO_3^-,0}$ that is calculated according to equation (8).

The equations make it possible to handle the inflow mass rates in two ways. The first one is to directly estimate the rates using the equations given source concentrations and assuming dimensions Y (such as a drain field width) and Z (a harder to assess source zone depth).

However, it requires specifying a uniform source plane height, Z, and results in inflow mass rates that vary for each septic system based on the specific estimate of the groundwater velocity for its flow path. When the height is difficult to estimate but the inflow mass rates can be estimated by other means (e.g., from literature or expert judgment), one can specify the nitrogen mass input rates M_{in}, the sum of $M_{NH_4^+,in}$ and $M_{NO_3^-,in}$, through ArcNLET user interface, and the code evaluates Z accordingly; the Z value is needed for estimating the cell volume used in equations (18) and (19). According to equations (20) – (21), M_{in} can be calculated for each plume as follows,

$$\begin{aligned} M_{in} &= \left(Y\theta v c_{NH_4^+,0} f_1 Z\right) + \left(Y\theta v a_{NO_3^-,0} f_2 Z - \frac{k_1}{k_1-k_2} \times Y\theta v c_{NH_4^+,0} f_1 Z\right) \\ &= \left(Y\theta v a_{NO_3^-,0} f_2 + \frac{-k_2}{k_1-k_2} Y\theta v c_{NH_4^+,0} f_1\right) Z \end{aligned} \tag{22}$$

where $k_2 = k_{deni}$, $k_1 = k_{nit}(1+\rho k_d/\theta)$

$$f_1 = \left(1 + \sqrt{1 + \frac{4k_{nit}(1+\rho k_d/\theta)\alpha_x}{v}}\right) \Big/ 2 \tag{23}$$

and

$$f_2 = \left(1 + \sqrt{1 + \frac{4k_{deni}\alpha_x}{v}}\right) \Big/ 2 \tag{24}$$

The source plan height, Z, is then calculated as,

$$Z = M_{in} \Big/ Y\theta v \left(a_{NO_3^-,0} f_2 + \frac{-k_2}{k_1-k_2} c_{NH_4^+,0} f_1\right) \tag{25}$$

The two options are implemented in the new ArcNLET and allow users to choose.

The simplified groundwater flow and nitrate transport model is implemented as an extension of ArcGIS using the Visual Basic .NET programming language. In keeping with the object oriented paradigm, the code project is structured in a modular fashion. Development of the graphical user interface (GUI) elements is separated from that of the model elements; further modularization is kept within the development of GUI and model sub-modules. The main panel of the model GUI is shown in Figure 2-2; there are four tabs, each of which represents a separate modeling component. For example, the tab of Groundwater Flow is for estimating magnitude and direction of groundwater flow velocity, and the tab of Particle Tracking for estimating flow path from each septic system. Each tab is designed to be a self-contained module and can be executed individually within ArcGIS. Five ArcGIS layers are needed for running ArcNLET. They are DEM, hydraulic conductivity, and porosity in raster form, septic system locations in point form, and surface water bodies in polygon form. These ArcGIS files need to be prepared outside ArcNLET. The output files are also ArcGIS layers that can be readily post-processed and visualized within ArcGIS. More details of the software development, including verification and validation, are described in Rios (2010) and Rios et al. (2013a).

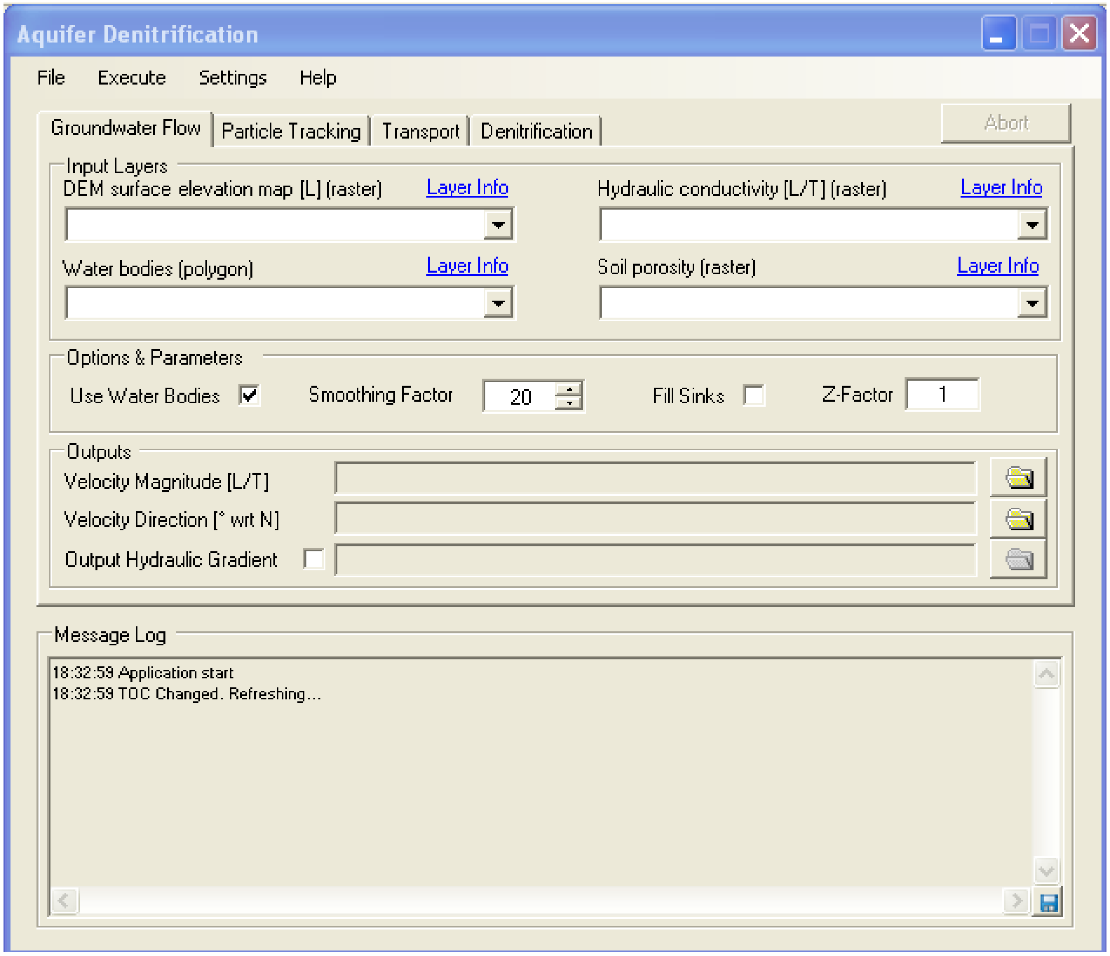

Figure 2-2. Main Graphic User Interface (GUI) of ArcNLET with four modules of Groundwater Flow, Particle Tracking, Transport, and Denitrification

Before ArcNLET is used for estimating nitrogen load to surface water bodies, calibrating the model parameters is always needed to match model simulations to field observations. However, in many projects of nitrogen pollution management, field observations are scarce. This is the reason of developing ArcNLET whose complexity is compatible with available data. As shown in the next section, observation data is extremely limited in the modeling area, and the conceptual model based on the limited data should be simple. On the other hand, the calibrated ArcNLET model is able to reasonably match field observations, as shown in Section 4.

3. ANALYSIS OF MONITORING DATA

This section analyzes the monitoring data compiled in this study to qualitatively evaluate potential impacts of septic systems on water quality (of surface water and groundwater) and to understand groundwater flow and nitrogen transport in the modeling areas. While there is a monitoring network of surface water quality, groundwater monitoring data is extremely limited in the modeling areas. This restricts development of complex conceptual models of groundwater flow and nitrogen transport, and leads to uncertainty in calibration of ArcNLET in the next section. Most of the data used in this section are downloaded from the SJRWMD, the EPA STORET (STOrage and RETrieval) database and the Hydrologic Information System managed by The Consortium of Universities for the Advancement of Hydrologic Science, Inc. (CUAHSI).

3.1. Hydrogeology and Hydrology in the Modeling area

The surficial aquifer system and the underlying Floridan aquifer system are the sources of all ground water used in Indian River County, Florida. The surficial aquifer system consists of a 100- to 150-foot-thick section of unconsolidated clastic deposits termed the "clastic zone" that overlies a 0- to 60-foot-thick section of mostly indurated carbonate rock termed the "shallow rock zone." The Floridan aquifer system consists of about 2,800 feet of carbonate rocks, subdivided on the basis of permeability, into the Upper Floridan aquifer (about 350-650 feet thick), the middle semi confining unit (about 20-120 feet thick), and the Lower Floridan aquifer (roughly 2,000 feet thick). The surficial and Floridan aquifer systems are separated by a 100- to 200-foot-thick low permeability rock unit known as the intermediate confining unit [Schiner et al. 1988].

Figures 3-1 plots the monthly and annual average precipitation at weather station VBA near the modeling areas, whose location is shown in Figure 3-2. The precipitation data are downloaded from SJRWMD. The observation period is from 01/01/2004 to 12/31/2013. Figure 3-1a shows that a wet season can be delineated from June to October; the smallest (33 mm) and largest (176 mm) monthly precipitation are in January and September, respectively. Figure 3-1b shows that the lowest and highest annual precipitations are 1317 mm in 2011 and 832 mm in 2006.

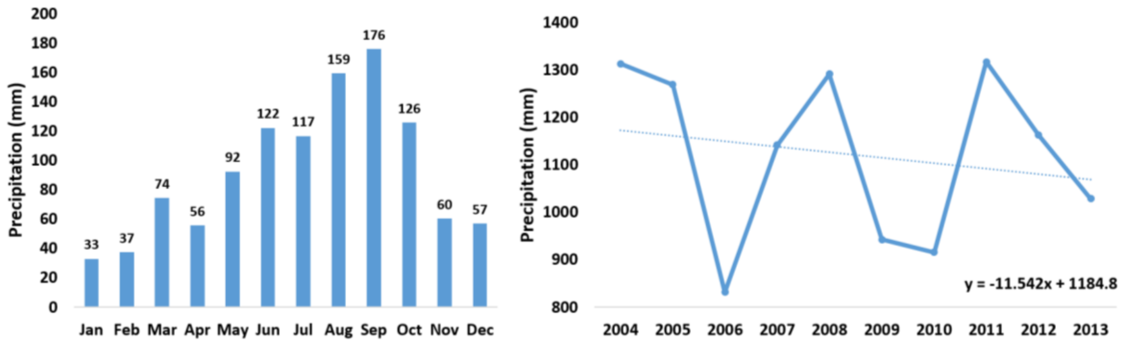

Figure 3-1. Monthly (left plot) and annual (right plot) average precipitation from 2004 to 2013 at weather station VBA (Vero Beach Airport), whose location is shown in Figure 3-2.

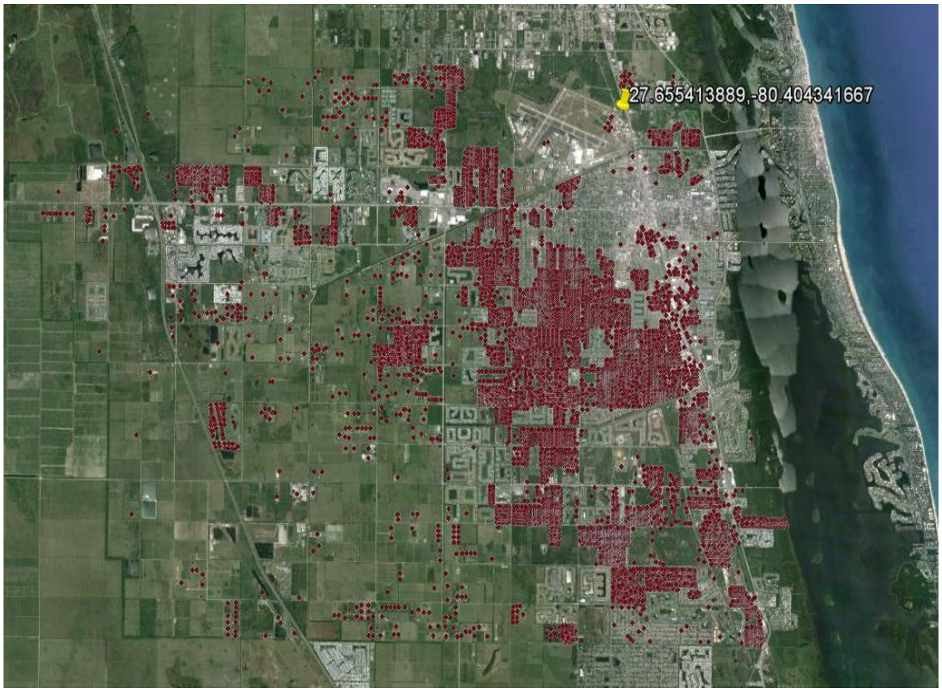

Figure 3-2. Locations of 12,741 active septic systems in the main-south canal drainage area (red). Location of the weather station (VBA), shown in yellow ribbon.

3.2. Active Septic Tanks

This study aims at conducting ArcNLET modeling to estimate nitrogen loads from removed septic systems to surface water bodies. Figure 3-3 shows the locations of 12,741 (red) active and 27,171(green) converted septic systems in the main-south canal drainage basins area (thick red and black lines). The septic system locations are provided by Arjuna Weragoda, Capital Projects Manager, IRC Department of Utility Services, Indian River County. It should be noted that the locations are not exact, but approximated by the geometric center of each parcel. Figure 3-4 shows the impaired waterbodies WBID3153A (main canal drainage basin) and WBID3158B (south canal drainage basin), which described in the BMAP (2012) generated by FDEP.

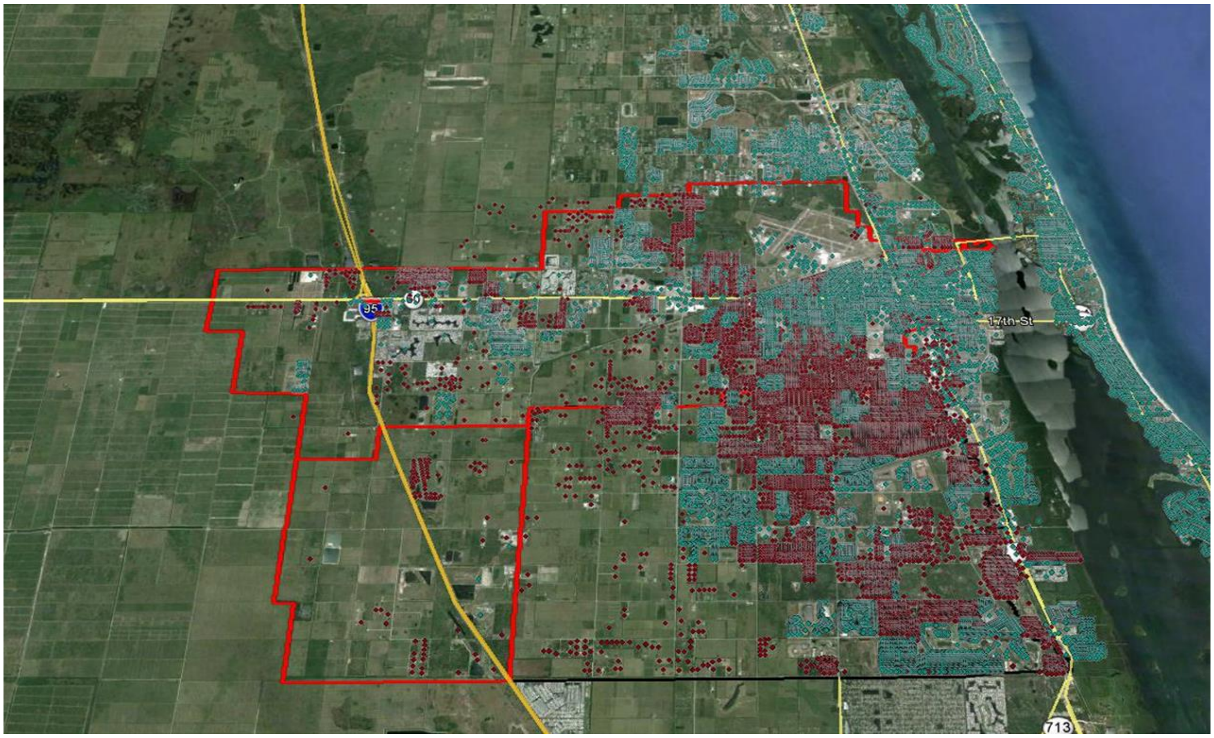

Figure 3-3. Locations of 12,741 (red) active and 27,171(green) converted septic systems in the main-south canal drainage area (thick red and black lines).

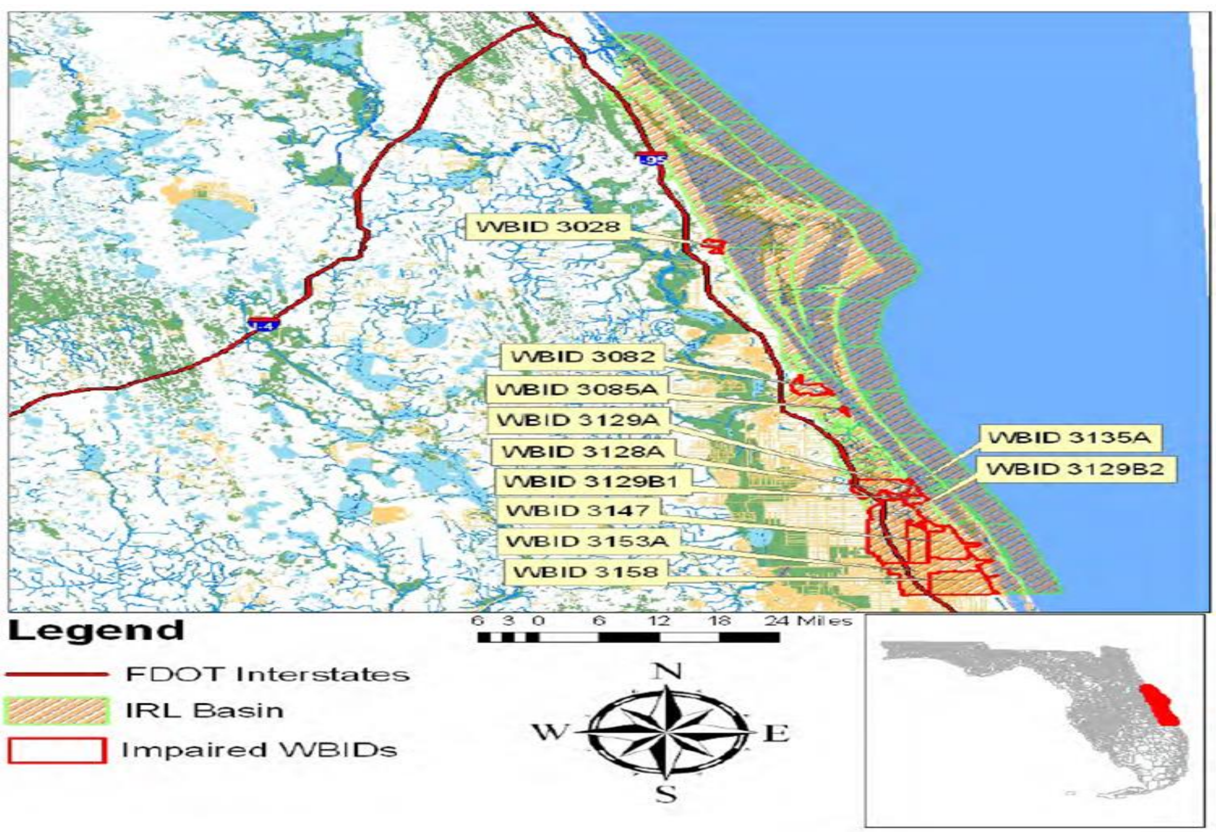

Figure 3-4 Impaired water bodies, adapted from BMAP report (2012).

3.3. Surface Water Quality

A network of surface water quality exists in the main-south canal drainage area (BMAP, 2013). Lemonteh Horne from FDEP provided the surface water quality data measured at 9 stations. The data from nine stations (Figure 3-5) located in the vicinity of septic tank area are analyzed here. Nine stations were separated in 3 stations of longer time records (from 1997 to 2013) in Figure 3-6 and 6 stations of shorter time records (only in 1 year) in Figure 3-7. Figure 3-6a-b shows the box plot of NOx and TN concentrations (mg/l) and figure 3-6c-e show the plotting's of time series of TKN, NOx and TN concentrations (mg/l). The TN and NOx concentrations ranges from 0.2- 2.1 mg/l and 0-0.45 mg/l, respectively, within the period of 1997 to 2013 (from figure 3-6a-b). For higher TKN concentration, TN concentrations exhibits the high concentration when compared with the NOx concentration. From the box plot it is also noticed that the median concentration in both NOx and TN are higher in IRLVSC when compared with the IRLVMC. It is expected because south canal drainage basin is densely populated and possess higher septic tank than the main canal.

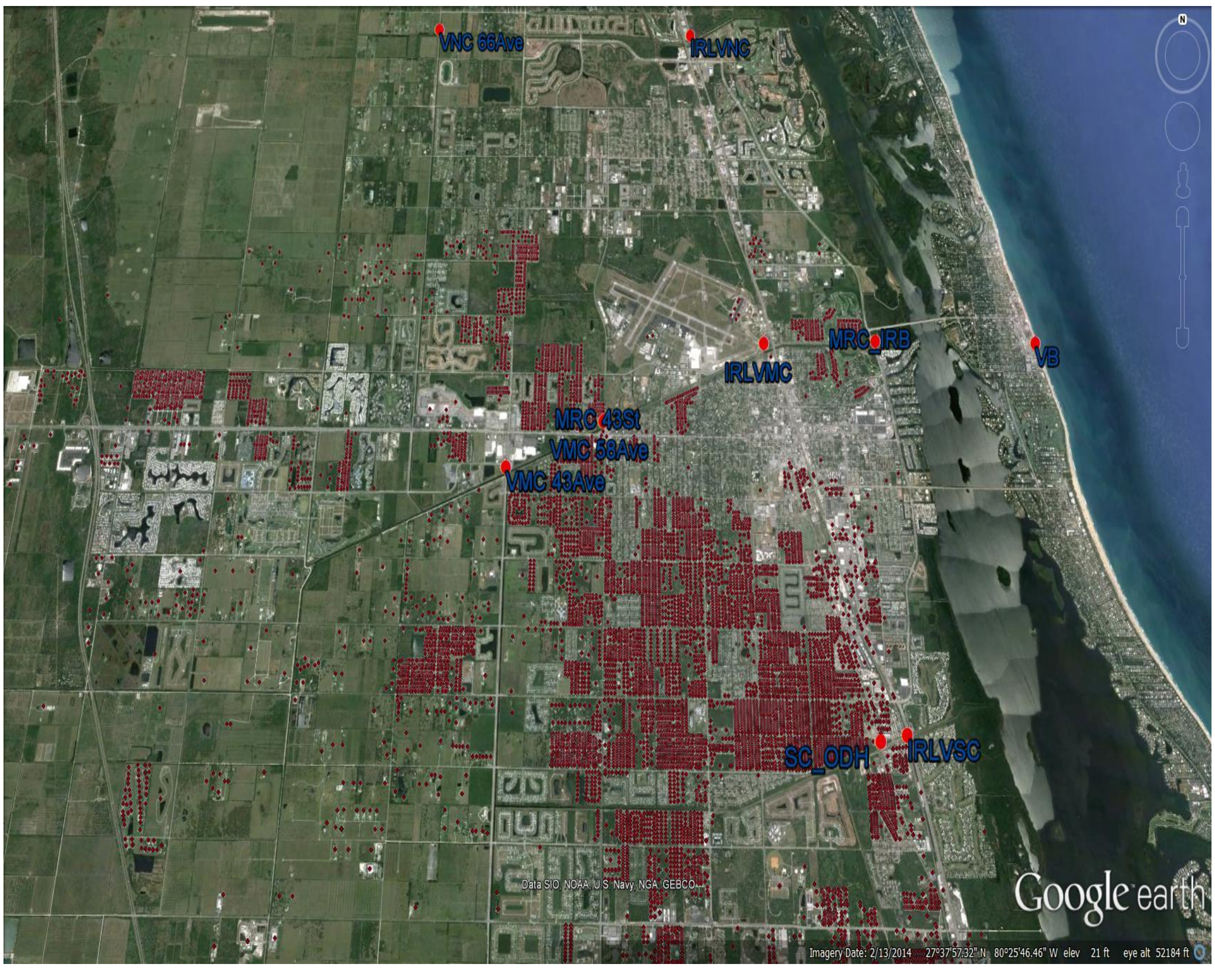

Figure 3-5. Locations of monitoring stations of surface water quality in the main-south canal drainage area (station names are labeled in blue).

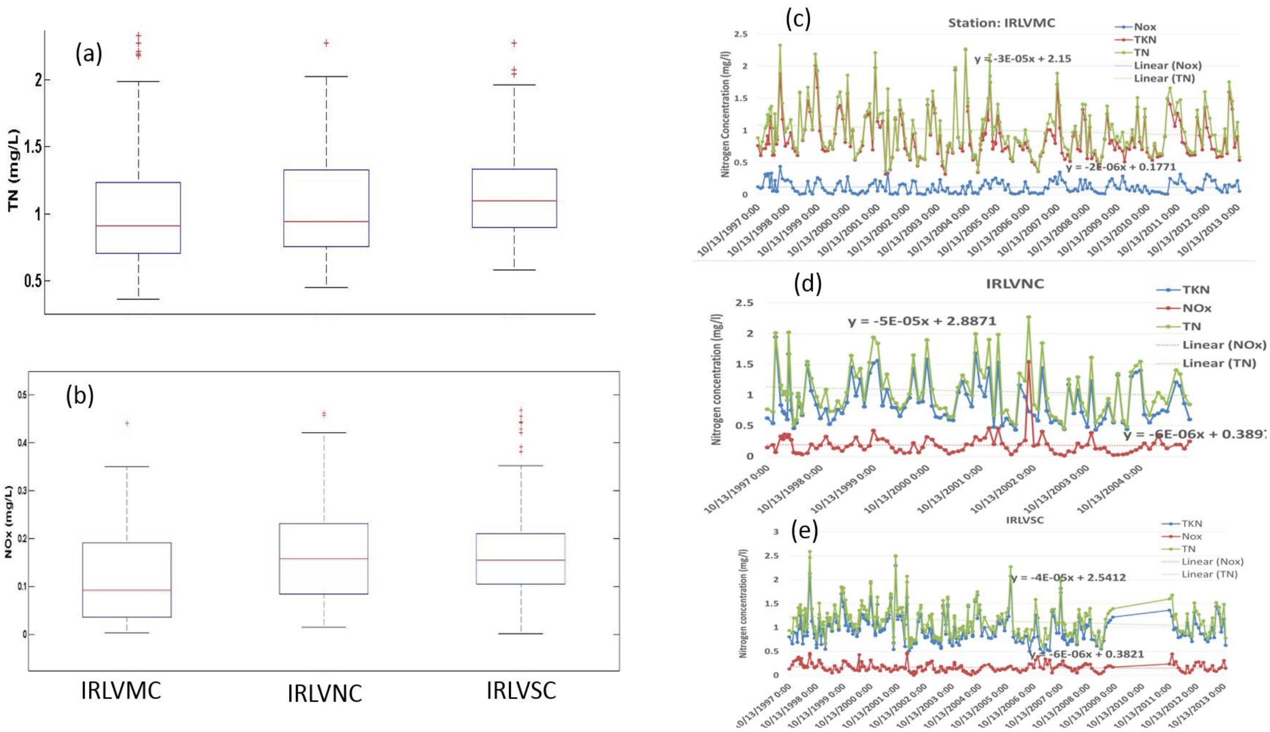

Figure 3-6. Box plot of a) TN (total nitrogen, b) NOx (nitrite and nitrate), c) Time series of the concentrations (mg/l) of TN, NOx, and TKN at IRLVMC, d) at IRLVNC, and e) at IRLVSC.

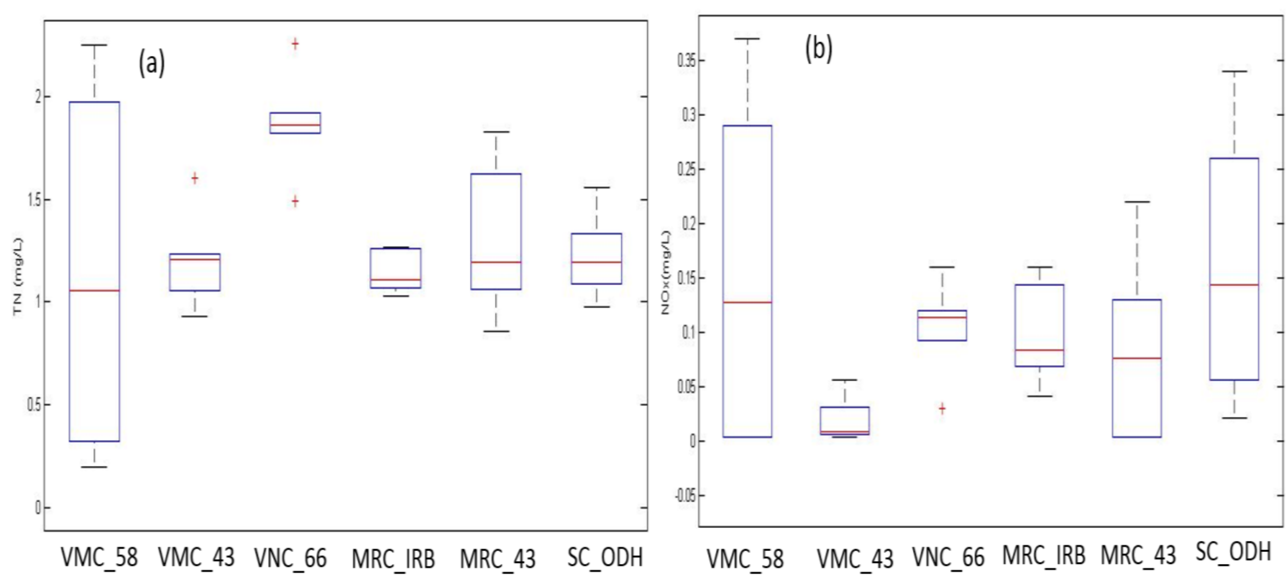

Figure 3-7. Box plot of a) TN (total nitrogen, b) NOx (nitrite and nitrate), c) Time series of the concentrations (mg/l) of TN, NOx, and TKN at IRLVMC, d) at IRLVNC, and e) at IRLVSC.

The time series plot in Figure 3-6c-e, show the high concentration of TKN and TN when compared with the NOx in 16 years in all the three stations. The zigzag shape shows the effects of seasonality. Linear decreasing trends found for all the three stations in all three species of nitrogen concentrations. This decreasing nitrogen concentration trends mean the improving water quality. This improvement should be relate to the projects of IRL have been implementing by the St. Johns River Water Management District's (SJRWMD) and Department of Environmental Protection (DEP) with the collaboration of other water control districts and agencies. Such as, C-1 re-diversion project, dragline ditch restoration, Conversion of On-Site Sewage Treatment and Disposal Systems (OSTDS) and storm water restoration through MS4, Non MS-4 etc [CCMP, 2008; BMAP, 2013].

Figure 3-7a and 3-7b shows the box plot of TN and NOx concentrations, respectively, in the year of 2003. The frequency of the datasets was 2 data/month. The VNC_66 station shows the highest median TN concentration and the SC_ODH shows the highest NOx concentration. From figure 3-5, VNC_66 is situated in the northern part of IRC, fertilizer from the agricultural land might be one of the reason of this high concentration when compared with other station. Again from figure 3-5, SC_ODH is situated the downstream of the south canal, which is surrounded by the densely population, could be one of the reason of high median NOx concentration.

3.4. Groundwater Data Selected to Calibrate ArcNLET Flow Model

Observations of groundwater levels are needed to calibrate the ArcNLET flow model by

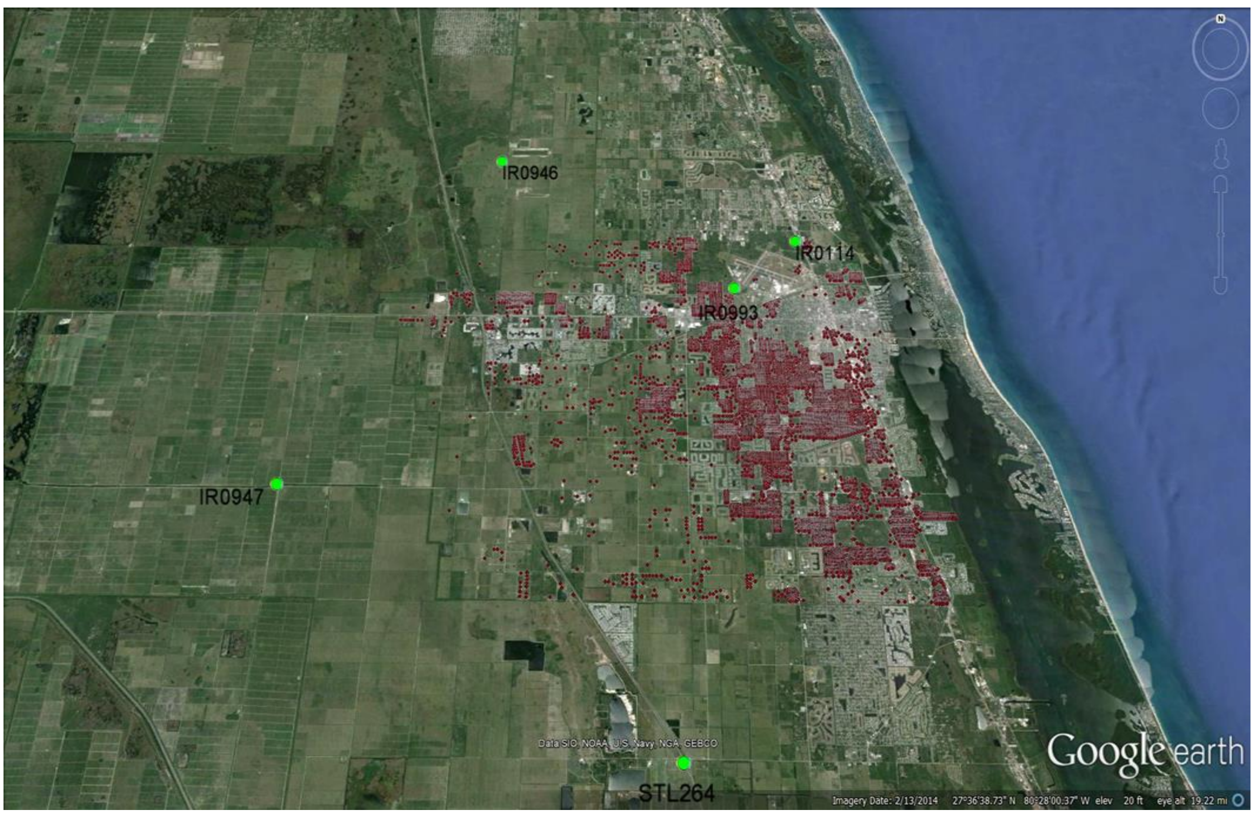

Figure 3-8. Location of Groundwater monitoring well

adjusting the smoothing factor so that the shape of smoothed DEM can match the shape of water table. Given that the flow model is a steady-state one, average (over time) water levels are used as the calibration target. A total of five monitoring wells are identified for the main-south canal. Figure 3-8 shows the five monitoring well locations. The wells IR0114, and IR0993 are withtin the septic systems located area, the wells IR0946, IR0947, and STL264 are within the peripheral of our modeling area, which should reflect the site specific hydrogeologic conditions. Due to the scarcity of the data within the modeling area, we have selected all the five monitoirng wells for our grounwater flow calibration in the smoothing process of

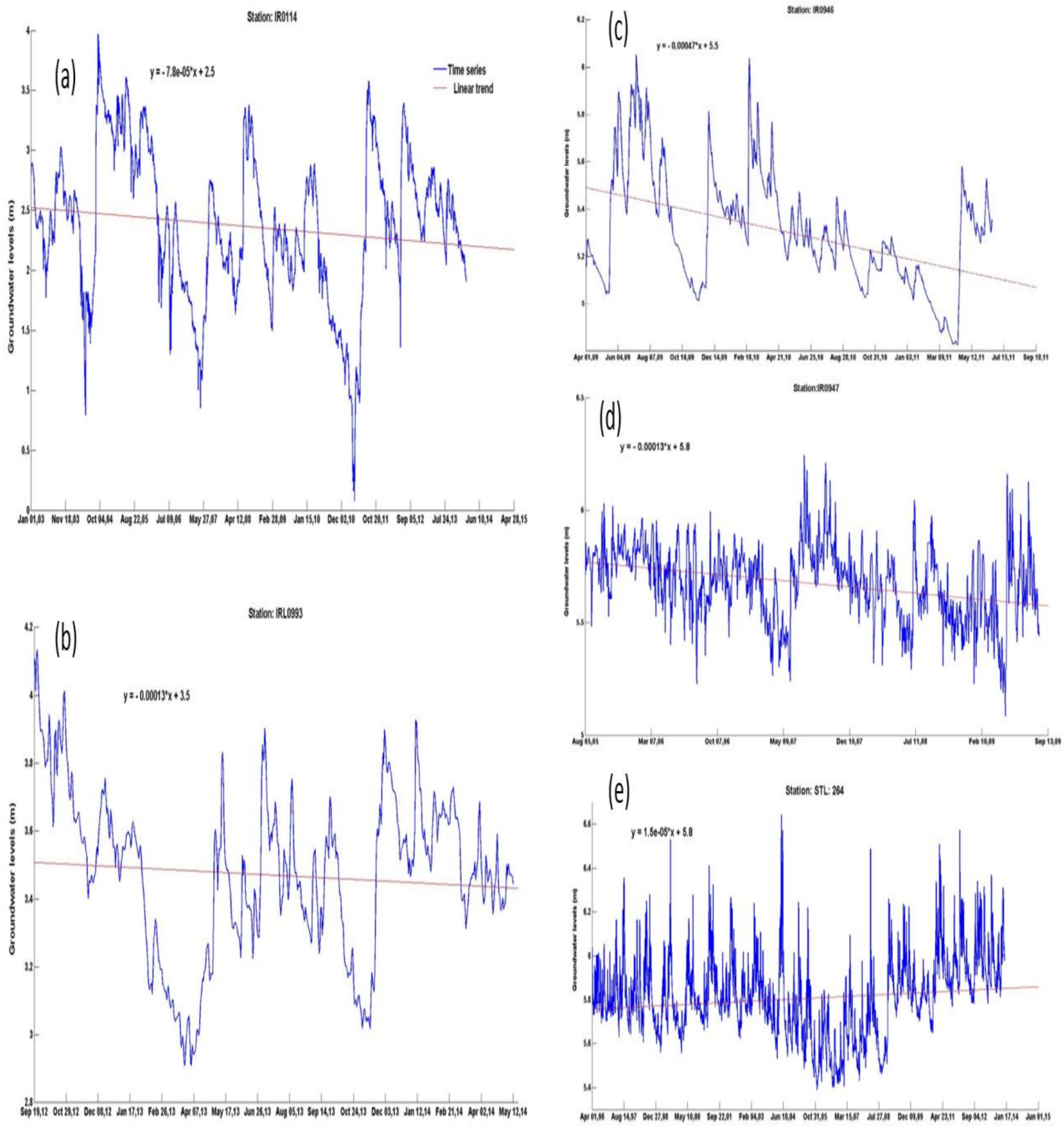

Figure 3-9. Location of Groundwater monitoring well

ArcNLET. These datasets were collected from the James Sylvania, FDEP. The periods and frequency of the datasets are not the same. Time series of the water level are plotted in Figure 3-9. Despite of moderate fluctuation, there is no apparent trend in the observations. Therefore, it is reasonable to use the average water level as the calibration target and to conduct steady-state ArcNLET modeling. Among the wells, mean water level in wells IR0114, and IR0993 are the lowest, less than 10 feet, approximately (Figure 3-9a and 3-9b). Mean water levels in well IR0946, IR0947, and STL264 are the highest, about 20 feet (approx.). The spatial trend of water level is consistent with that of land surface elevation (descresing from west to east), suggesting that it is reasonable to assume that water table is a subdued replica of topography.

3.5. Analysis of Nitrogen Concentration Data

Observations of nitrogen concentration are extremely scarce. Data are compiled from James Sylvania, FDEP. Locations of the five monitoring wells used in the study are shown in Figure 3-10. Figure 3-11 shows the ammonia and NO_x concentrations in different time periods at

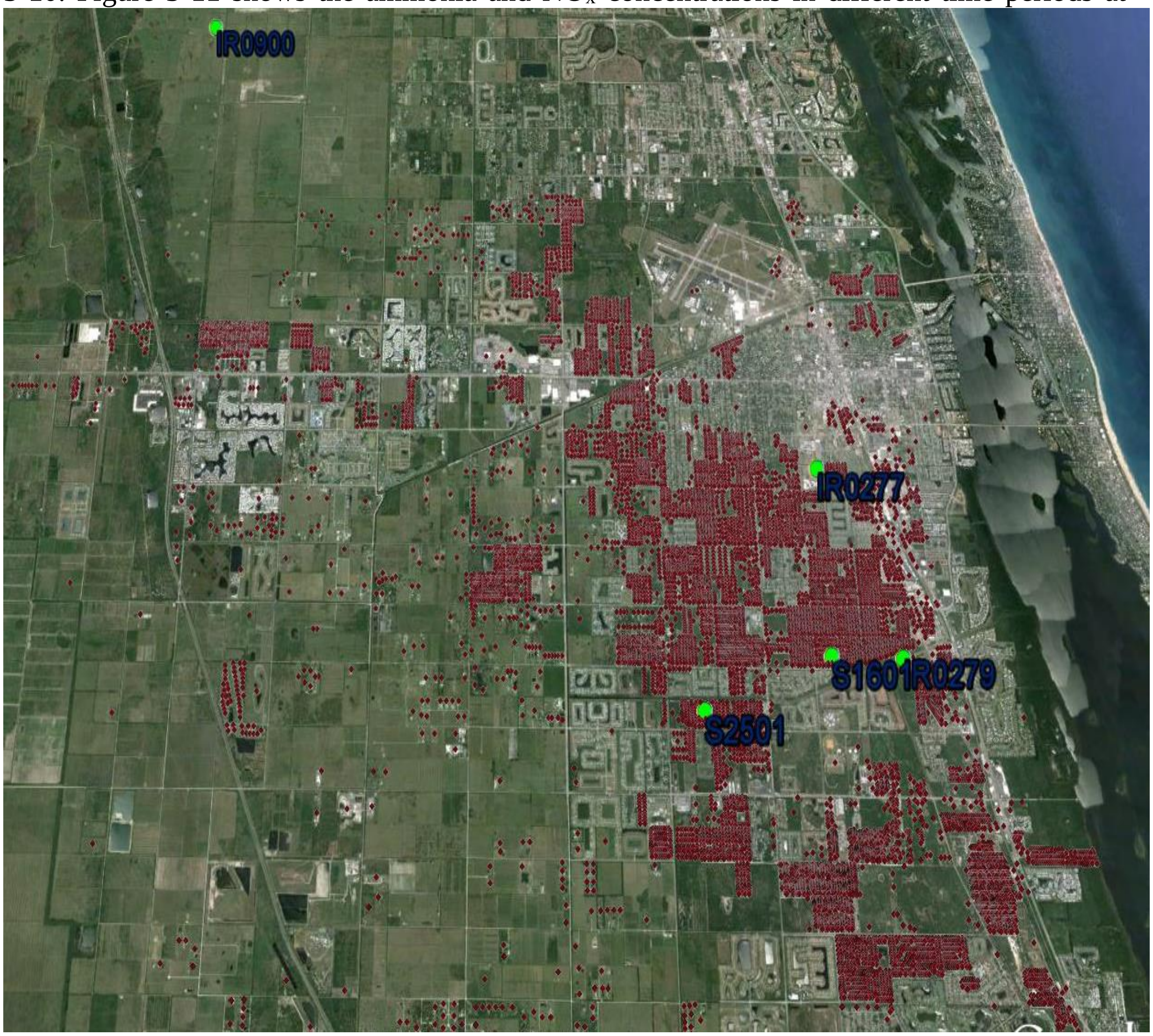

Figure 3-10. Location of groundwater monitoring well

different monitoring locations. The NO_x concentrations are significantly smaller than ammonium concentrations, regardless of the sampling depths.

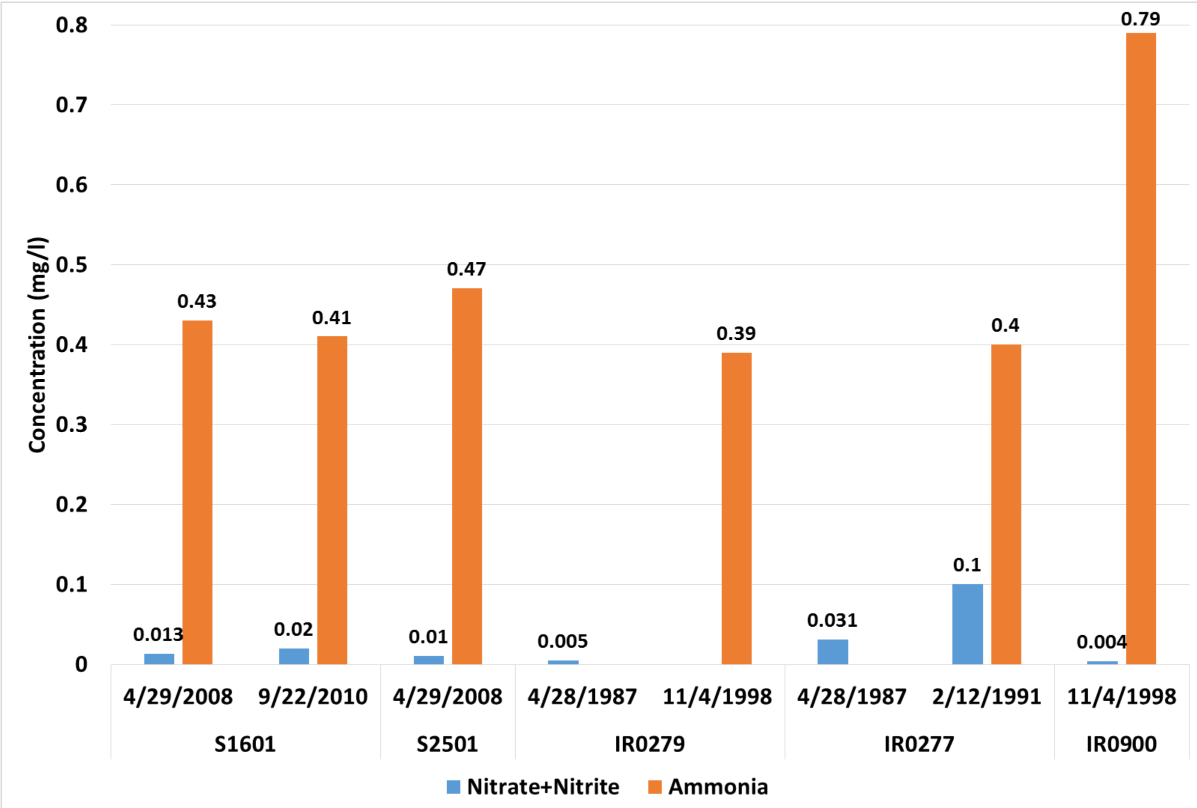

Figure 3-11. Nitrogen concentration (mg/l) data of five monitoring well

4. ARCNLET MODEL SETUP, CALIBRATION, AND LOAD ESTIMATION

This section starts with a brief description of the data needed for ArcNLET modeling in Section 4.1, followed by identification of calibrated parameters of the ArcNLET model in Section 4.2. Model calibration results for the main-south canal drainage basin is given in Sections 4.3., and the load estimates are evaluated in Section 4.4. At last, the estimates are discussed in the BMAP context in Section 4.6 to provide an example of using the ArcNLET load estimates in support of BMAP and TMDL implementation.

4.1. Data Needed for ArcNLET Modeling

Data needed for ArcNLET modeling include DEM, locations of removed septic systems, locations of surface water bodies, and values and spatial distributions of hydraulic conductivity and porosity. These data are collected with assistance of colleagues at FDEP, the Indian River County, and the other sources. The data need to be prepared in the ArcGIS data format so that they can be used directly by ArcNLET. The basic procedure of preparing the data is given below; more details of the procedure are referred to ArcNLET user's manual (Rios et al., 2011a) and application manual (Wang et al., 2011). The site-specific transport parameter values (e.g., source plane concentration, dispersivities, and first-order decay coefficient of denitrification) are not available but obtained by model calibration as described in Section 4.2.

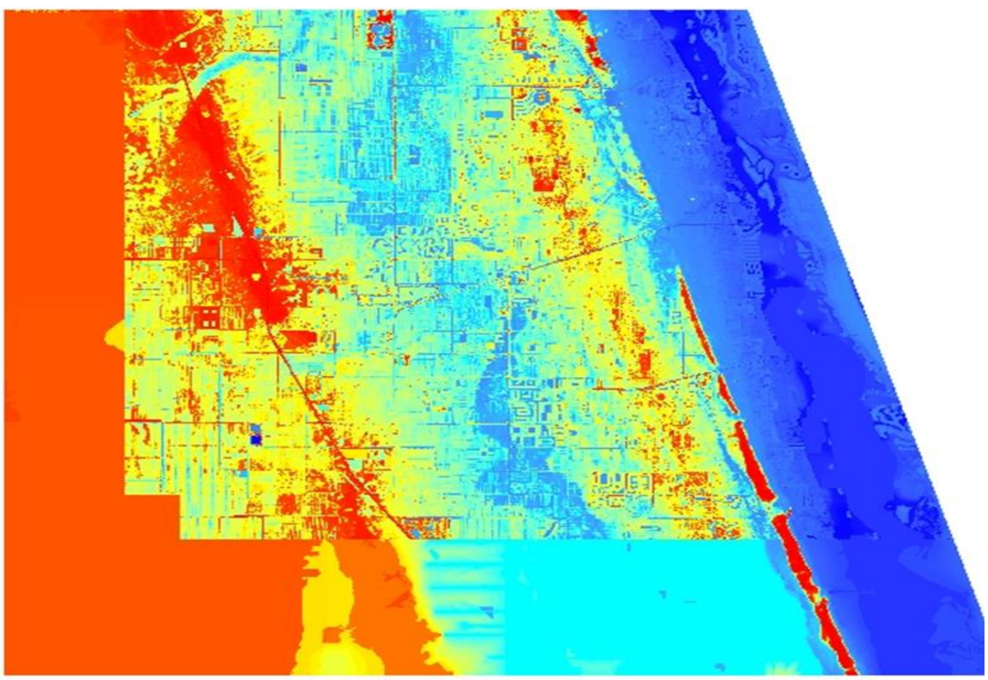

Figure 4-1. LiDAR DEM with resolution of 15×15 feet2 in the middle main modeling area and regular DEM with resolution of 10×10 m2.

The DEM data used in this study includes LiDAR DEM and regular DEM. The LiDAR DEM with resolution of 15 × 15 feet^2 is downloaded from SJRWMD's GIS Data Catalog (http://floridaswater.com/gisdevelopment/docs/themes.html). For the rest of the modeling area where the LiDAR DEM is unavailable, regular DEM with the resolution of 10 × 10 m^2 is downloaded from the USGS's National Elevation Dataset (http://ned.usgs.gov/). By applying the mosaic function, the LiDAR DEM and the regular DEM are merged together with the resolution of 10 × 10 m^2. The final DEM used in this study is shown in Figure 4-1. It should be noted that the low resolution of the regular DEM affects accuracy of the numerical simulation, because it cannot reveal spatial variability at the scale smaller than 10 ×10 m^2, the DEM resolution. However, high computational time require in ArcNLET when dealing with the finer resolution DEM.

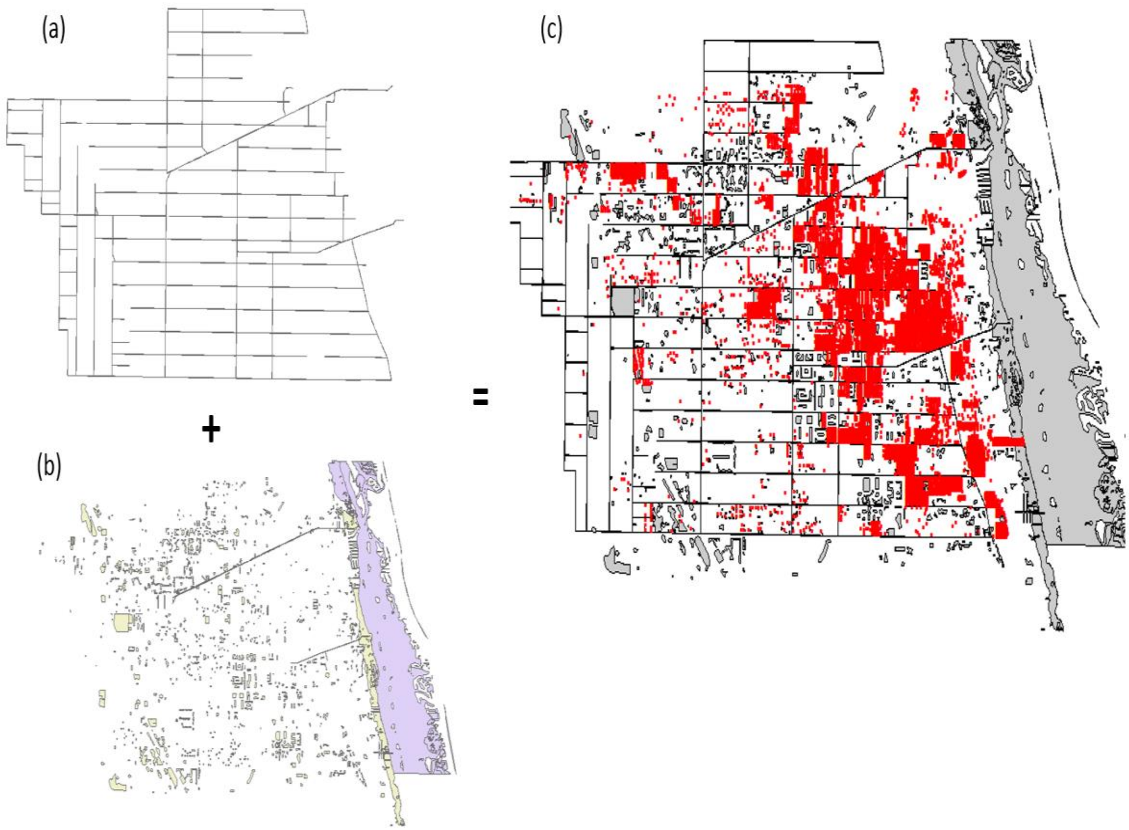

Figure 4-2. ArcGIS files of (a) canals and (b) ponds, rivers, lakes, and swamps/marshes, (c) merged and complete water bodies in the modeling area. Septic systems are shown in red color.

The locations of surface water bodies are obtained from two sources: (1) the USGS National Hydrography Dataset (NHD, http://nhd.usgs.gov/) for all the modeling areas, and (2) the canal data of the main-south canal drainage basin area provided by Will Rice, IRC. Note that the flow lines in the NHD database are not useful to ArcNLET modeling, because the lines do not have width. Thus, NHD flow line data was not useful and we had to rely on the IRCs canal data with the width information. The NHD waterbodies data and IRC provided canal data are merged to form the final ArcGIS layer of complete surface water bodies, which is shown in Figure 4-3c for this modeling.

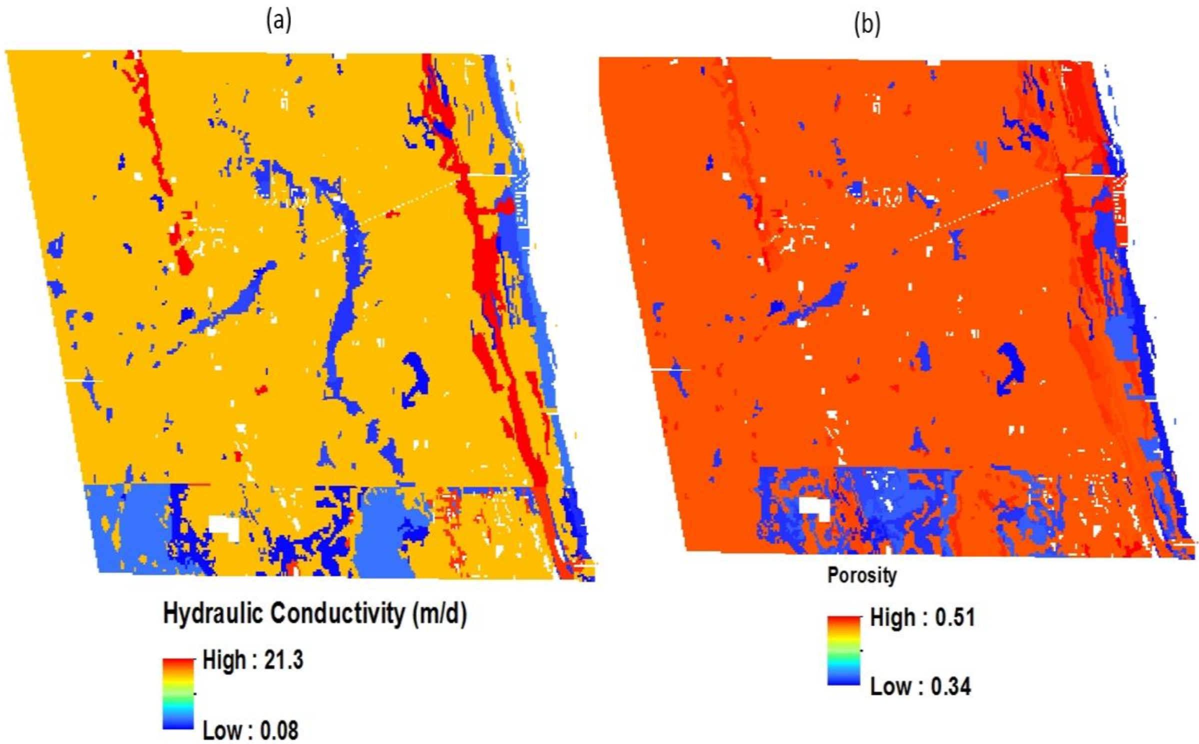

Figure 4-3. Spatial distribution of (a) hydraulic conductivity (m/d), and (b) porosity generated from the SSURGO soil database for the main-south canal drainage basin.

Three steps are needed to prepare hydraulic conductivity and porosity data for ArcNLET modeling. The first step is to download the soil data for the modeling area from the SSURGO soil database (http://soils.usda.gov/survey/geography/ssurgo). Subsequently, the polygons of heterogeneous hydraulic conductivity, and porosity are generated by aggregating soil data from horizons to components and then to units. Afterward, by using the "polygon to raster" function of ArcGIS, the polygon file of hydraulic conductivity and porosity are converted into a raster file used by ArcNLET. The details of these operations are referred to Wang et al. (2011). The resulting raster file of hydraulic conductivity and porosity data for this modeling area is shown in Figure 4-4a and 4-4b, respectively.

4.2. Calibrated and Uncalibrated ArcNLET Model Parameters

Following Wang et al. (2011, 2013), calibration of ArcNLET model is conducted by manually adjusting model parameters to match smoothed DEM values to observed hydraulic heads for the ArcNLET flow model and to match simulated nitrogen concentrations to observed concentrations for the ArcNLET transport model. The details of the calibration data of hydraulic head and nitrate concentration are given in Section 4.3.

The calibrated ArcNLET parameters are the smoothing factor, source plan concentration (C_0), longitudinal dispersivity (α_L), horizontal transverse dispersivity (α_{TH}), and first-order decay coefficient of denitrification (k). Table 4-1 lists the initial values and ranges of the parameters obtained from literature and our previous experience of using ArcNLET. The reasons of selecting the initial value and the ranges are as follows:

(1) **Smoothing factor**. This parameter is specific to ArcNLET. It is used to smooth DEM to generate the shape of the water table. During the calibration, this parameter value is adjusted so that a 1:1 slope between observed hydraulic heads and corresponding smoothed DEMs can be obtained. A larger value of smoothing factor results in a smoother shape of the water table and thus smaller hydraulic gradient. The parameter is site specific and strongly correlated to site topography. A fine resolution of topography requires a large value of smoothing factor. Rios (2010) tested several smoothing factors for a groundwater model developed for the U.S Naval Air Station (NAS) in Jacksonville. The groundwater model was calibrated by Davis et al. (1996) and the calibrated water table was used as the reference to evaluate the best smoothing factor. It was found that a value of 50 yielded a good approximation to the water table (Rios, 2010). Therefore, the initial value is set as the average value of 50. The smoothing factor is assumed to follow uniform distribution and the range is set as 20 ~ 80 empirically.

(2) **Source plane concentration** (C_0). Nitrogen enters groundwater through the source plan shown in Figure 2-1. As shown in equation (11), the simulated nitrogen concentration is linearly proportional to C_0. There is no field measurement of this parameter value in the modeling areas. A review article of McCray et al. (2005) suggested a range of 25~80 mg/L. Valiela et al. (1997) gave the value of 44 mg/L. A value of total nitrogen concentration of 39 mg/L at the edge of the drainfield was assumed for conventional septic systems (U.S. EPA, 2013). For conventional septic tanks in Florida, an average concentration of 45 mg/L was estimated in Wakulla (Harden et al., 2010) and 35 mg/L of total nitrogen was estimated in Santa Fe River Basin (BMAP, 2012). The value of 45 mg/L is used as the initial value.

(3) **Longitudinal dispersivity (α_L)**. There is no field measurement of this parameter, and literature values are used. While Dann (1996) used the range of 1.2 ~ 7.5 m for α_L in Pinellas County in Florida, Merritt (1996) gave a calibrated value of 76 m for the Biscayne aquifer in Florida. In Gelhar et al. (1992), a range between 6 and 170 m was reported. Therefore, a range of 1 ~100m is set for α_L in this study, and the initial value is 10 m, which was obtained in the ArcNLET modeling by Wang et al. (2013).

(4) **Horizontal transverse dispersivity (α_{TH})**. While the ratio between α_L and α_{TH} is 10 as a rule of thumb, the ratio varies at different sites (Rehfeldt, et al, 1992). For example Merritt (1996) calibrated the two parameters at the Biscayne aquifer and obtained 76 m and 0.03 m for α_L and α_{TH}, respectively. Ratios between 5:1 and 100:1 have been reported in literature (Delgado, 2007). Therefore, α_{TH} is taken as 1/5 ~ 1/100 of α_L. The initial value is set as 1m, 1/10 of the initial value of α_L.

(5) **First-order decay coefficient of denitrification (k)**. There is no site-specific measurement of this parameter in the modeling areas. Tesoriero and Puckett (2011) gave a range of 5.4×10^{-5} ~ 7.3×10^{-4} d^{-1} for shallow aquifers. It is significantly smaller

than the range of 0.004 ~ 2.27 d^{-1} given in McCray et al. (2005). Since the soil organic carbon in the SSURGO database is low (2.014% and 1.129% for Port St. Lucie and Stuart, respectively), it is reasonable to set a small range for the parameter. According to the model calibration of Wang et al. (2012), the maximum value of 0.015 d^{-1} is used, and range is 5.4×10^{-5} ~ 0.015 d^{-1}. The initial value is taken as 0.005 d^{-1}, which was obtained in the ArcNLET modeling by Wang et al. (2013).

The initial values are not critical, as the parameter values are adjusted during the calibration. The ranges can be adjusted if more data and information bring more information of the parameters.

Table 4-1. Ranges, initial values, and calibrated values of ArcNLET model parameters.

Parameter	**Range**	**Initial Value**	**Calibrated values**
Smoothing factor	20 to 80	50	65
C_0 (mg/L)	25 ~ 80	45	40
α_L (m)	1 ~ 100	10	1
α_{TH} (m)	1/5 ~ 1/100 of α_L	1	0.1
k (d^{-1})	5.4×10^{-5} ~ 0.015	0.001	0.00055

The un-calibrated parameters are hydraulic conductivity, porosity, and the inflow mass (M_{in} (g/d) of equation 22) from a septic system to groundwater. In ArcNLET modeling, there are two equivalent ways of handling the inflow mass: (1) to fix M_{in} and evaluate Z using equation 22 (Z is the source plan height needed for calculating the mass of denitrification and load), and (2) to fix Z and calculate M_{in} using equation 22. In this study, the first option is used, and the value of inflow mass is approximated as nitrogen release per person per day (4.8 kg/yr, a review value in Table 5 from Valiela et al. (1997)) × people/house (2.5 on average according recent census data) × 0.7 (not lost in septic tanks and leach fields, according to a report of MACTEC, 2007). The number of 2.5 people per house is the average of 2.4 and 2.6 people per house in Martin and St. Lucie counties (census data available at http://quickfacts.census.gov/qfd/states/12/12061.html). Therefore, the input mass from septic to groundwater is 8.4 kg/yr, i.e., 23.0 g/d. This estimate is larger than the most literature values listed in Table 4-2 but close to 21.7 g/d reported in the Wekiva study (Roeder, 2008). It is also close to the value of 22.4 g/d calculated according to Anderson (2006) as 11.2 g/person/d × 2.34 persons/household × 80% not lost in failed septic systems. This value is used for all the individual septic systems in the modeling sites. Site-specific M_{in} should be used if it can be estimated using site-specific data and information. While the M_{in} value is not calibrated, its estimate is subject to large uncertainty. In the study of Geay (2004), this value ranges from 4.2 to 10.7 kg/yr, because nitrogen reduction rate in septic tanks and drainfields is an uncertain variable. Although the value of 30% (MACTEC, 2007) obtained from the Wekiva study of the Florida Department of Health is used here, the rate is between 25% and 50% in the three sites of the Wekiva study (Roeder, 2008).

Table 4-2. Daily nitrogen loadings per household (g/d) from septic system to groundwater reported in literature and in this study.

Reference	Site Location	Daily N load per household
Koppelman, 1978[a]	Long Island, NY	15.8
Gold et al., 1990[a]	Kingston, RI	21.9
Weiskel and Howes 1991[a]	Buzzards Bay, MA	11.0-18.5
Maizel et al., 1997[a]	Chesapeake Bay	16.4-24.0
Valiela et al., 1997[a]	Waquoit Bay, MA	19.9
Reay, 2004[a]	Coastal Plain, VA	16.4-19.9
Roeder, 2008	Wekiva, FL	21.7
This study	St. Lucie Estuary, FL	23.0

Note: [a] Calculated by multiplying 2.5 persons/houshold to daily nitrogen loadings per person converted from annual loading per person listed in Table 3 of Reay (2004).

4.3. Calibration of ArcNLET Flow and Transport Models

The ArcNLET flow model is calibrated by adjusting the smoothing factor to match the shape of smoothed DEM and the water table. The calibration results are plotted in Figures 4-4. The locations of monitoring wells for the water table are shown in Figure 3-8; discussion of the calibration data is given in Section 3.4-3.5. For the calibration at the two sites, the starting value of smoothing factor is 80 and ranges 20-80, and the calibrated value is 65 (Table 4-1). As shown in Figure 4-4, the slopes of the linear regression lines between smoothed DEM and water table are close to 1 (0.936), and the R^2 values of the linear regression are significant 0.82.

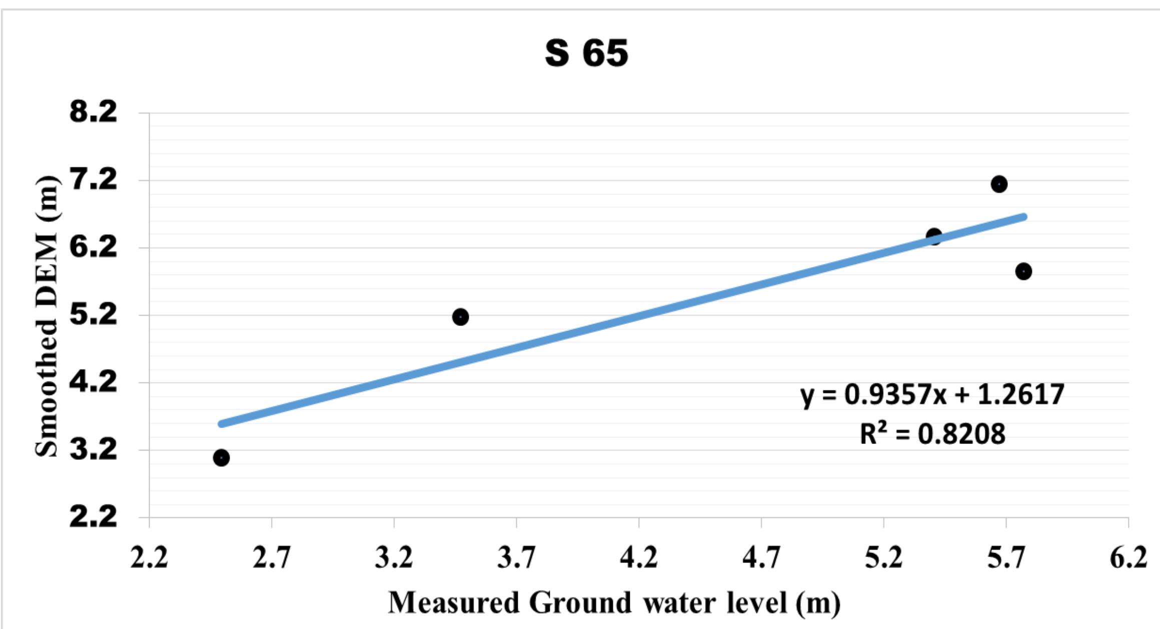

Figure 4-4. Smoothed DEM and measured water level at the modeling area.

The ArcNLET transport model is calibrated by adjusting the values of source plane concentration, longitudinal dispersivity, horizontal transverse dispersivity, and first-order decay coefficient of denitrification. The septic tank files used for the calibration are prepared in the way described in Section 4.1. The calibrated parameter values for the modeling area is listed in Table 4-1. The difference may result in different spatial distributions of simulated plumes. Generally speaking, large values of longitudinal dispersivity correspond to long plumes, and large values of horizontal transverse dispersivity to wide plumes.

Figure 4-5 plots the simulated and measured nitrogen concentrations at the two monitoring wells (S1601, and S2501) for the modeling area. The other three wells were excluded because of the outside of the plume boundary. Figure 4-5 shows the three well calibrated line, which all has the R^2=1.

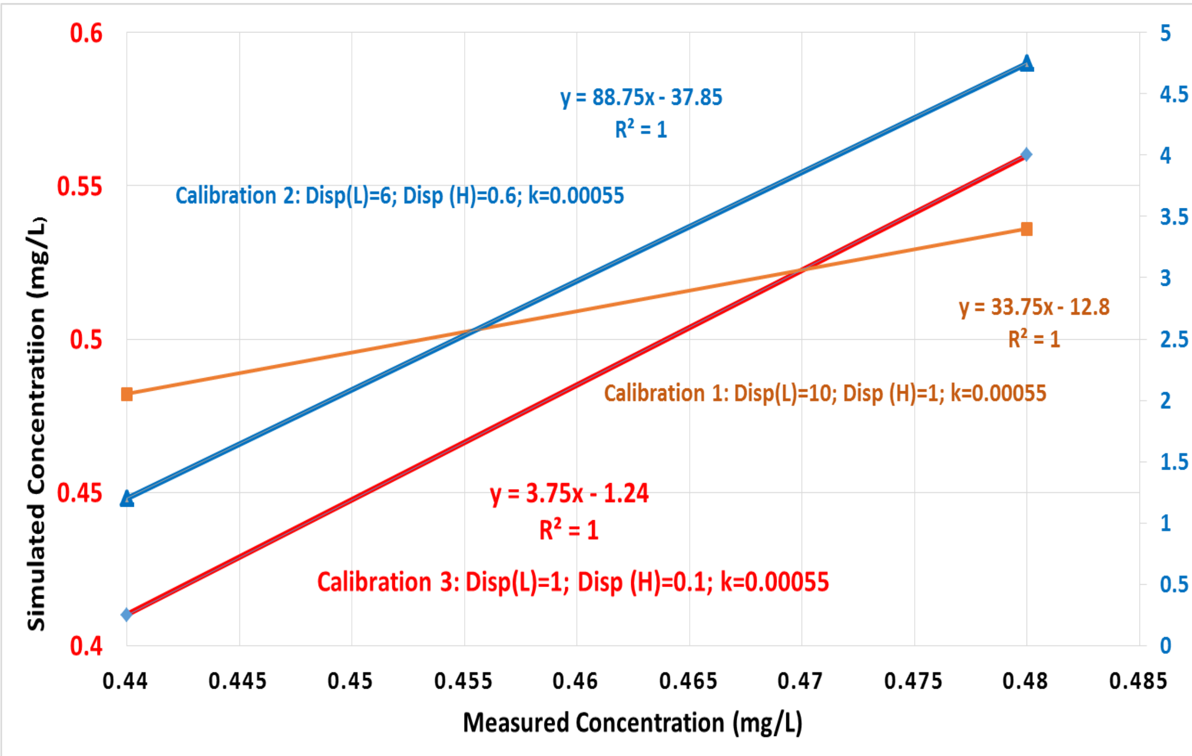

Figure 4-5. Simulated and measured concentrations at two wells (S1601, and S2501) shown in Figure 3-10(location) and Figure 3-11(concentrations) for the modeling area.

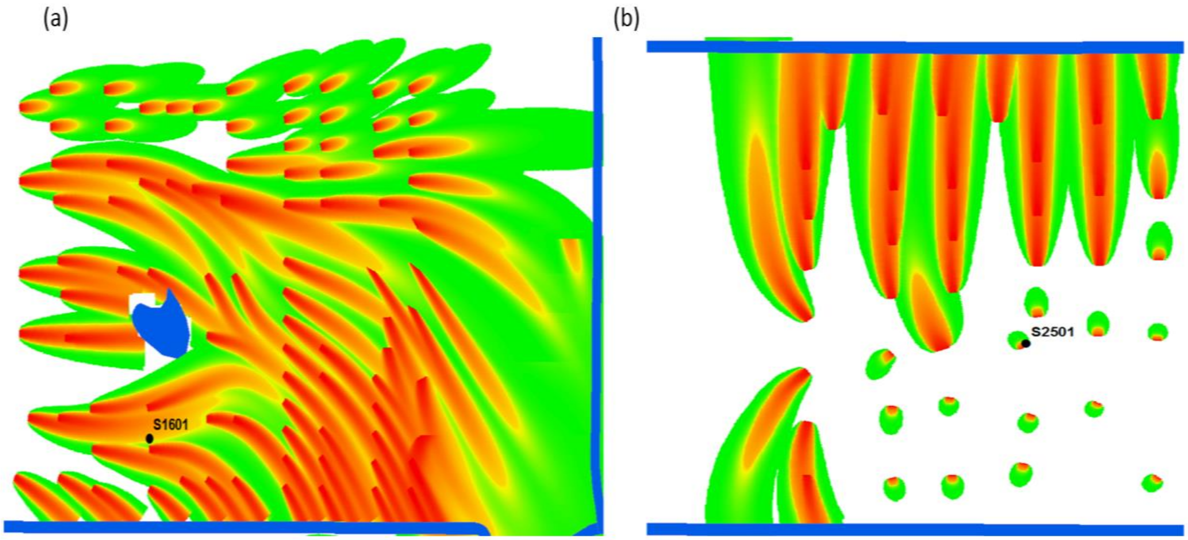

Figure 4-6. Simulated plumes by the calibrated ArcNLET model in the modeling area around wells (a) S1601, and (b) S2501. Surface water bodies are plotted in blue.

4.4. Nitrogen Load Estimation

The calibrated parameters listed in Table 4-1 are used to estimate nitrogen load from the active septic systems in the main-south canal drainage area.

4.4.1. Nitrogen Load Estimation for the main-south canal drainage area

Figure 4-7 plots the simulated flow paths from the active septic systems to surface water bodies. The canals (Figure 4-3) are important to determine groundwater flow direction, because groundwater discharges to nearby canals, not directly to the Lagoon. Figure 4-8 depicts the simulated nitrogen plumes from the active septic systems. The estimated load from 12,741 septic systems in the entire modeling area is 13742 lbs/yr. The load estimates and the number of contributing septic systems to the individual water bodies are listed in Appendix A. The nitrogen load per septic system is 2.56 g/d. The removal ratio due to denitrification is 85.0. This ratio is comparable to those reported in the literature, and more discussion is given in Section 4.5.

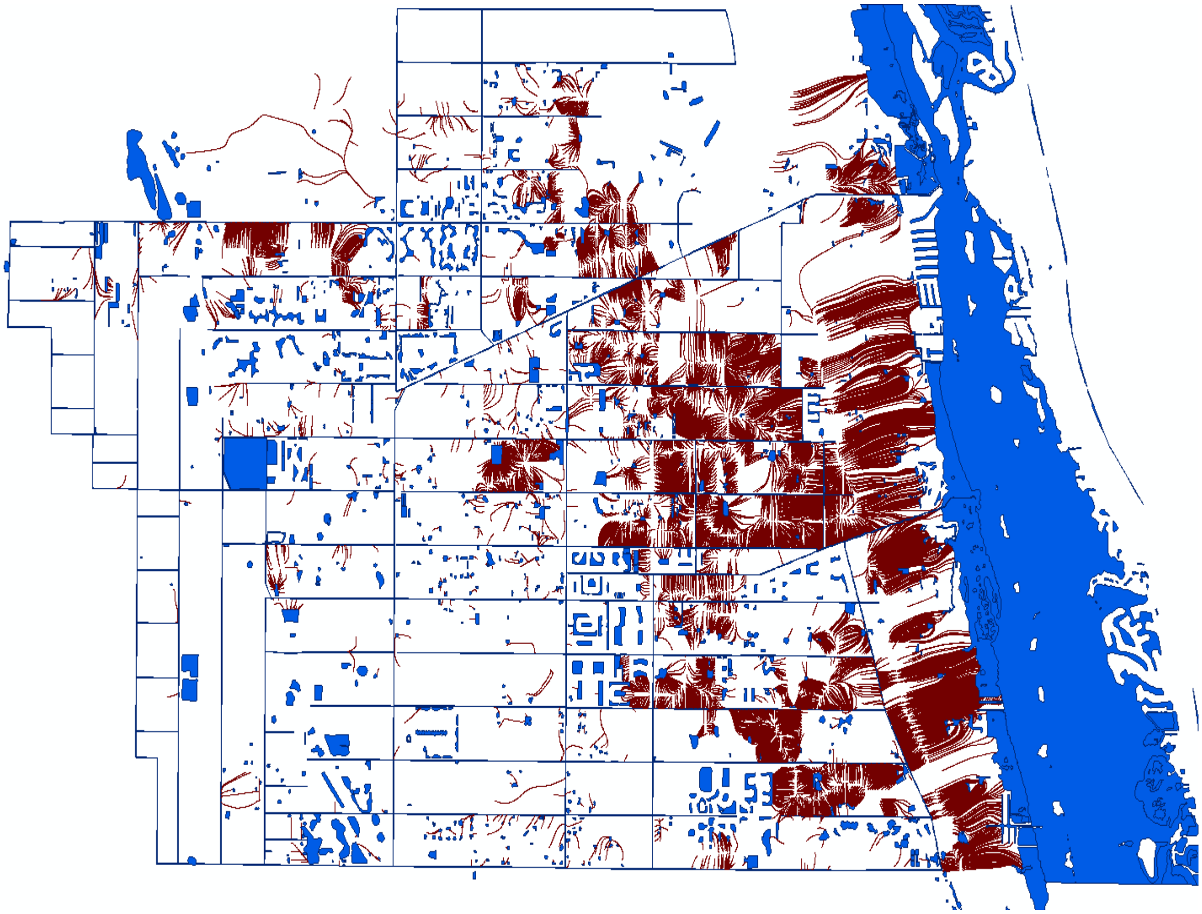

Figure 4-7. Simulated flow paths from active septic systems to surface water bodies in the main-south canal drainage area.

Figure 4-8 depicts the simulated nitrogen plumes from the removed septic systems. The canal is the longest water body, which receives more nitrogen load than any other waterbodies in the vicinity of the modeling area. Figure 4-9a shows the highest 20 load receiving waterbodies (waterbody FIDs were shown in x-axis) and Figure 4-9b shows the location of that waterbodies (waterbody FIDs were written in dark black). In Figure 4-9a, percentage of total load contribution is shown in secondary axis and blue color in the bar. Highest 20 waterbodies receive 6802 lbs/year (50.5% of total load), which is contributed by the 22% septic systems. These percentages suggest that reducing nitrogen load to a small number of surface waterbodies (20 out of 1100) can help reducing nitrogen load to the entire modeling area. The detailed of the highest load contributor (amount and location) makes it possible for environmental managers to determine areas with high priority of septic removal in planning of future removal.

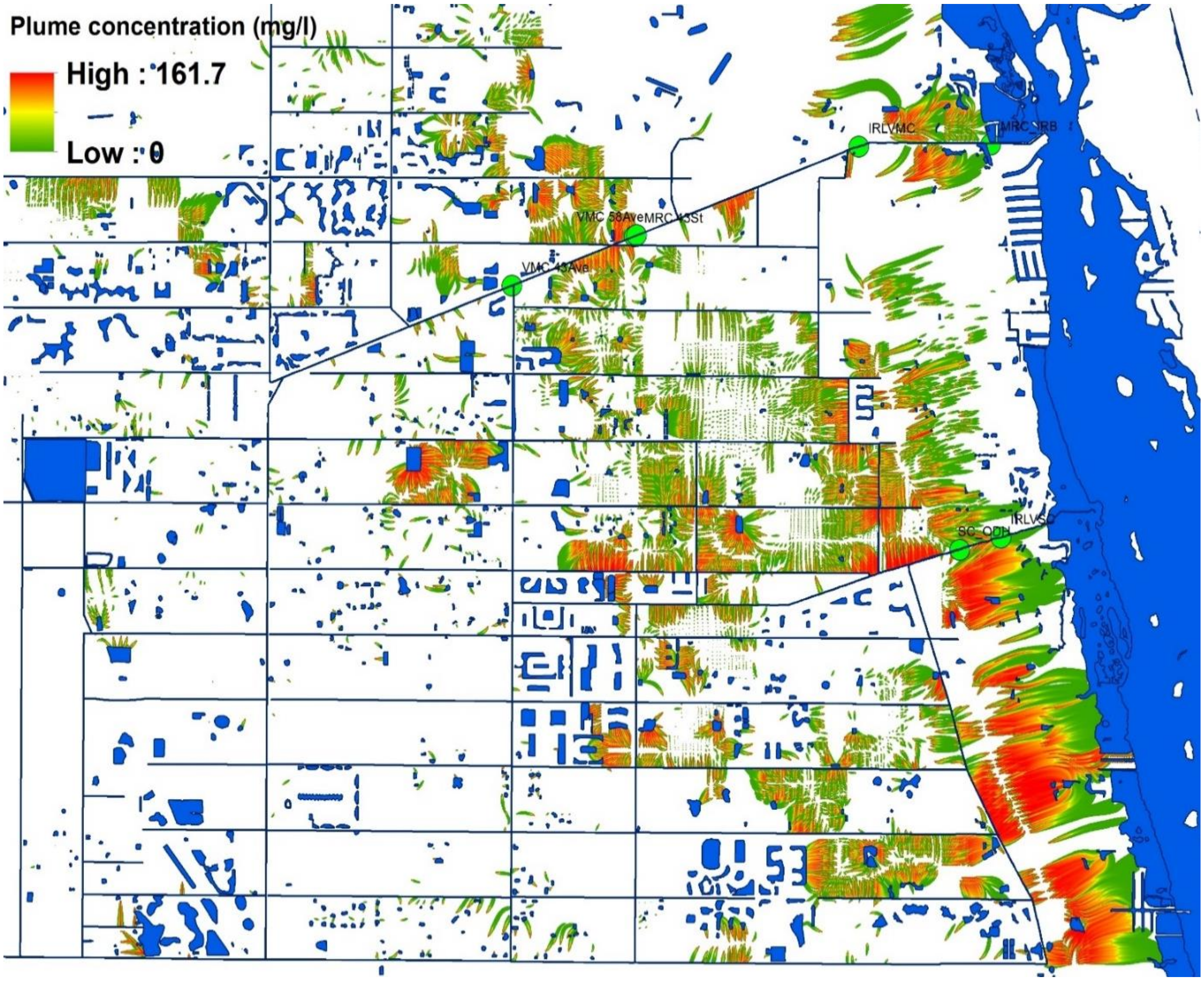

Figure 4-8. Simulated nitrogen plumes from the active septic systems in the main-south canal drainage area.

Indian River Lagoon (IRL) receives less nitrogen loadings than canals because of the distance from the septic system. In the NHD database, the IRL is separated into eight water bodies (Figure 4-10b), and the estimated load to each segment of the lagoon is shown in Figure 4-10a. Table 4-3 present the detailed of nitrogen load contributed to the Indian River Lagoon (IRL). It is noticeable that 2% of total load has been received by the IRL connected waterbodies. This is very insignificant.

Figure 4-11 shows a linear relation between the median values of surface water nitrogen concentration and logarithm of the nitrogen loads to the surface water bodies. It suggests that nitrogen load from septic systems to surface water bodies is one of the reasons for deterioration of surface water quality. This analysis also illustrates that the spatial variability revealed in the ArcNLET modeling results is useful to nitrogen contaminant management. Table 4-4 lists the median nitrogen concentration at the fourteen monitoring stations and the groundwater nitrogen load per unit length along the water bodies corresponding to the monitoring stations.

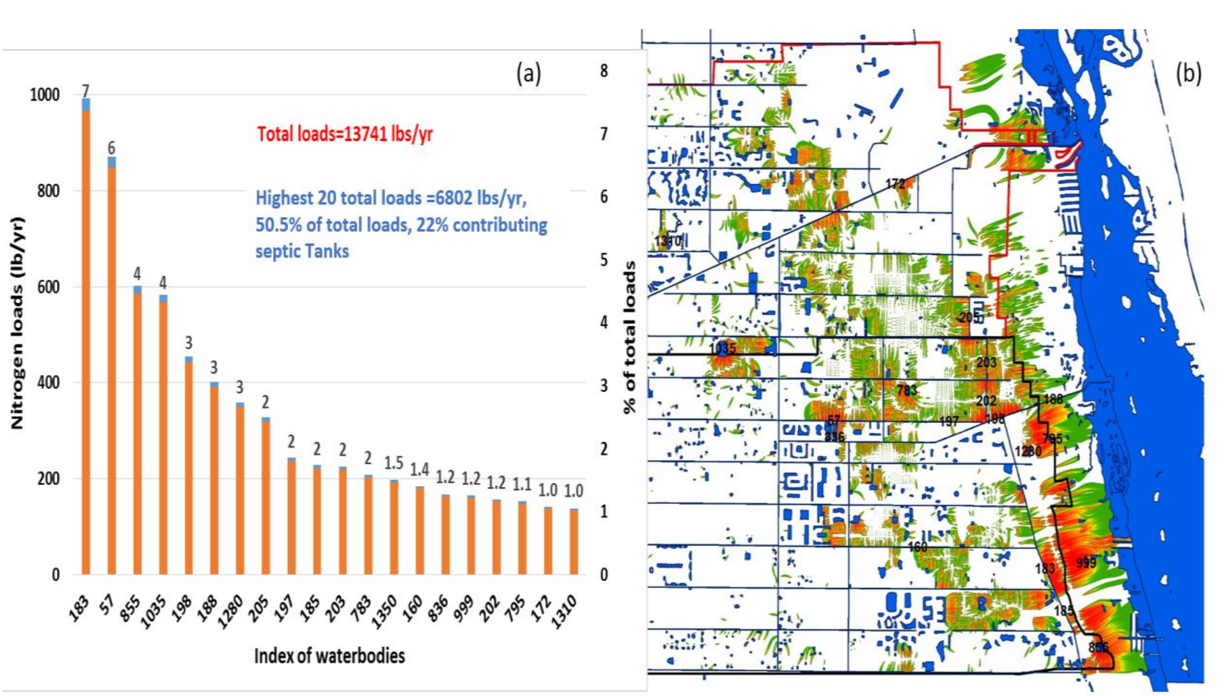

Figure 4-9. Highest loadings of 20 waterbodies that received 50.5% of total nitrogen loads (a) chronologically shown the nitrogen loads (lb/yr) with the index of waterbodies in x-axis, and (b) nitrogen plumes with the waterbodies location marked and written in black ink from the active septic systems in the main-south canal drainage area.

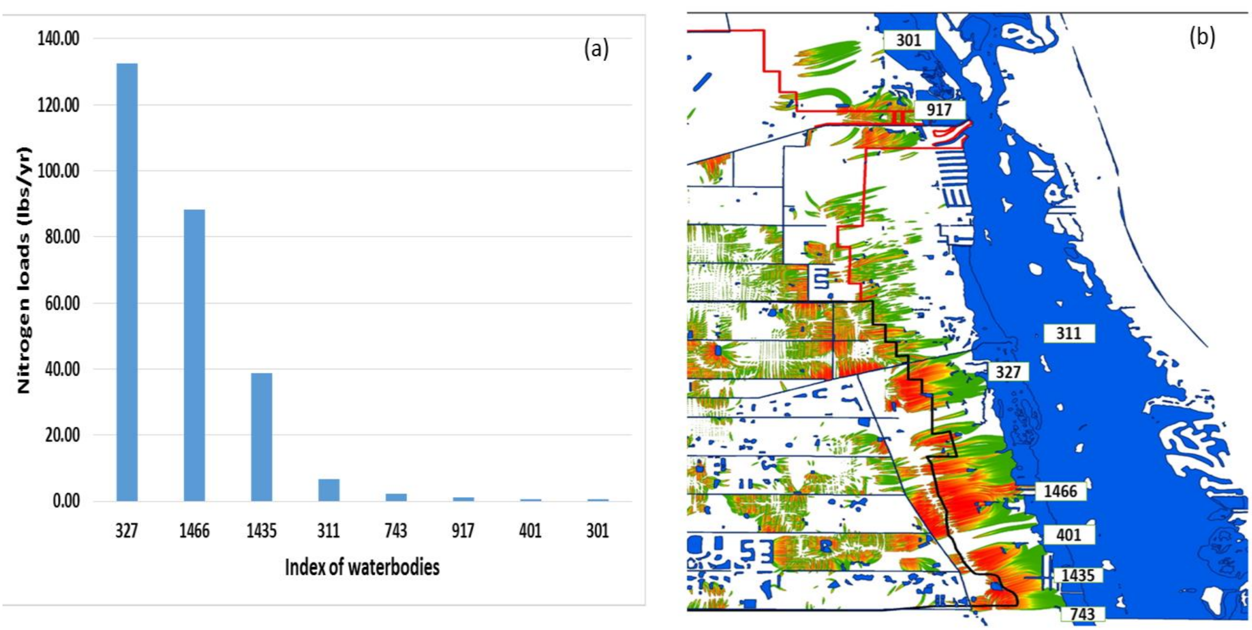

Figure 4-10. Indian River Lagoon receives the nitrogen loads from the connected waterbodies (a) chronologically shown the nitrogen loads (lb/yr) with the index of waterbodies in x-axis, and (b) nitrogen plumes with the waterbodies location marked and written in black ink from the active septic systems in the main-south canal drainage area.

Table 4-3. Nitrogen load contributed to the Indian River Lagoon (IRL). Location of these waterbodies were shown in Figure 4-10b.

WBID	load (mg/d)	load (lb/yr)	contributed septic tank	total loads to IRL	% of total load
327	164794.4	132.63	223	270.98	2.01
1466	109618	88.22	10		
1435	48060.2	38.68	45		
311	8378.91	6.74	2		
743	2831.59	2.28	37		
917	1401.7	1.13	11		
401	842.59	0.68	11		
301	771.37	0.62	19		
Total	336698.76	270.98	358		

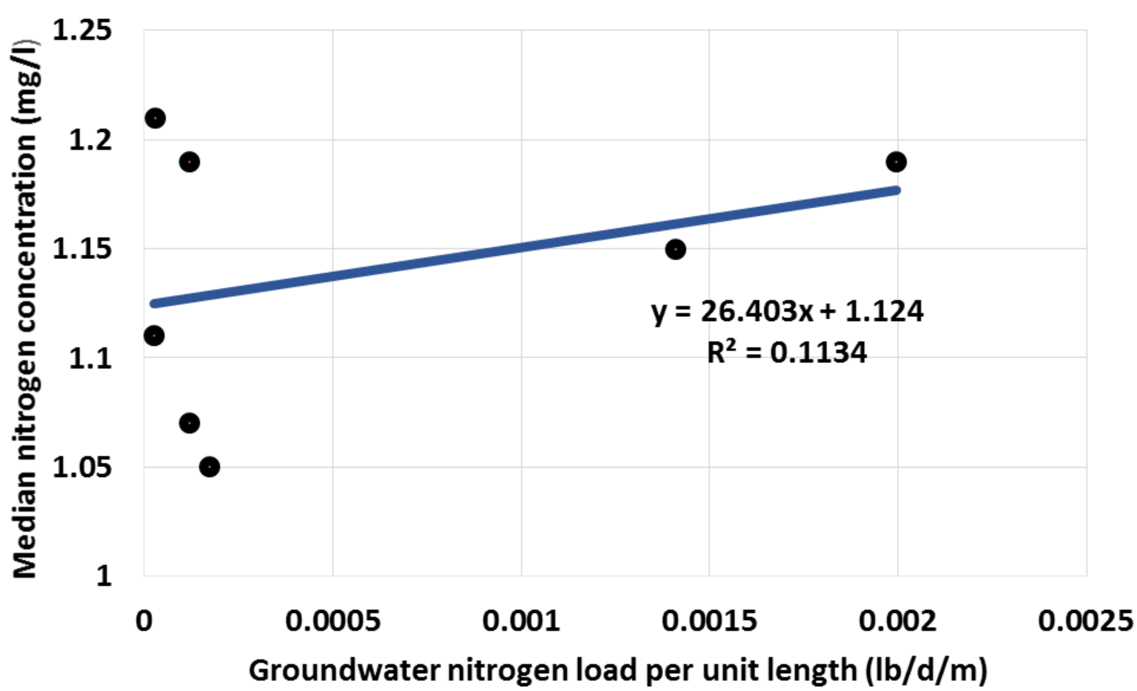

Figure 4-71. Median nitrogen concentration at seven monitoring stations and groundwater nitrogen load per unit length along the water bodies corresponding to the monitoring stations. The x-axis is in the logarithm scale.

Table 4-4. Median nitrogen concentration of surface water and estimated groundwater nitrogen load to the water bodies corresponding to monitoring stations of surface water. Monitoring stations were shown in Figure 4-8.

Monitoring Station	Surface Water nitrogen Concentrations (mg/l)	FID of WaterBodies corresponding to Stations	Length of Water Bodies (m)	Nitrogen load to Water Bodies (kg/d)	Nitrogen Load per unit length (kg/d/m)
VMC 43 Ave	1.21	102	1472	0.019	1.2908E-05
MRC 43 St	1.19	55	375.65	0.021	5.4664E-05
VMC 58 Ave	1.07	55	375.65	0.021	5.4664E-05
IRLVMC	1.05	215_1	191	0.015	7.8534E-05
MRC_IRB	1.11	215	1961	0.024	1.2326E-05
SC_ODH	1.19	198, 188_1	1171	1.06	0.00090521
IRLVSC	1.15	198,188	1705	1.09	0.00063945

The water bodies with the top ten largest load estimates are labeled with their FIDs in Figure 4-14, and the estimated loads and numbers of contributing septic systems are listed in Table 4-5. The sum of the load estimates is 24.3% of the total load, and the sum of the contributing septic systems is 20.5% of the total number of removed septic systems. In addition, Table 4-5 shows that, while the largest load estimate corresponds to the largest number of contributing septic systems, a large number of contributing systems does not necessarily lead to large nitrogen load. For example, the load from 112 septic systems to water body 352 is smaller than the load from 88 septic systems to water body 445. This is not surprising, because the load estimation depends on groundwater flow, solute transport, denitrification, and travel distance and time from septic systems. In other words, the load estimation should not be based on the number of septic systems but needs to consider spatial variability of flow and transport conditions in the modeling areas.

4.5. Evaluation of the ArcNLET Estimated Nitrogen Loads

The ideal way to evaluate the load estimates is to compare them with the corresponding field measurements. This however is impossible due to lack of field-scale load measurements. Instead, the load estimates are evaluated by identifying controlling factors of the load estimates, comparing the estimates with literature data of annual load per hectare and nitrogen reduction ratio and with the load estimates of another method used by Martin County. For the convenience of discussion, the total loada, numera of septic tanks, and loada per septic system for the seven modeling sites are listed in Table 4-5.

Table 4-5. Main and South canal drainage basins contributed load, and load per septic system.

	Area (acre)	No of Septic tanks	lbs/yr	lbs/yr/septicTank
Main canal	24666	5346	4548.73	0.85
South Canal	15122	7395	8922.25	1.21
Total	39788	**12741**	**13470.98**	**1.06**

4.5.1. Controlling factors of load estimate

It is found in this study that the amount of load estimate is controlled by the following physical factors: length of flow paths, flow velocity, and drainage condition. The length of flow paths is important, because longer flow paths result in more denitrification and thus smaller load estimate. Figure 4-21 plots the load estimates with the mean lengths of flow paths at the seven modeling sites of this study (for each septic system, the length of flow path is from the septic system to receiving surface water body). The two largest loads per septic systems are for North River Shores and Seagate Harbor where the flow paths are the shortest (Figures 4-16 and 4-17). The relation between mean length of flow path and nitrogen load is also reported in Meile et al. (2010). Therefore, in the management of nitrogen pollution, it is important to consider spatial variability of the distance between septic systems and surface water bodies as implemented in ArcNLET.

Figure 4-22 plots variation of the load estimate with the mean velocity at the seven modeling site. It shows that the load estimate increases with the mean velocity. This is reasonable, since larger flow velocity corresponds to shorter travel time and thus smaller amount of denitrification and larger amount of load. Figures 4-21 and 4-22 indicate that the setback distance in nitrogen pollution management should be determined not only by the distance between septic systems to surface water bodies but also by groundwater flow conditions. However, in comparison with the mean length of flow paths, the flow conditions may play a secondary role, since variation of the mean velocity is small, as shown in Figure 4-22.

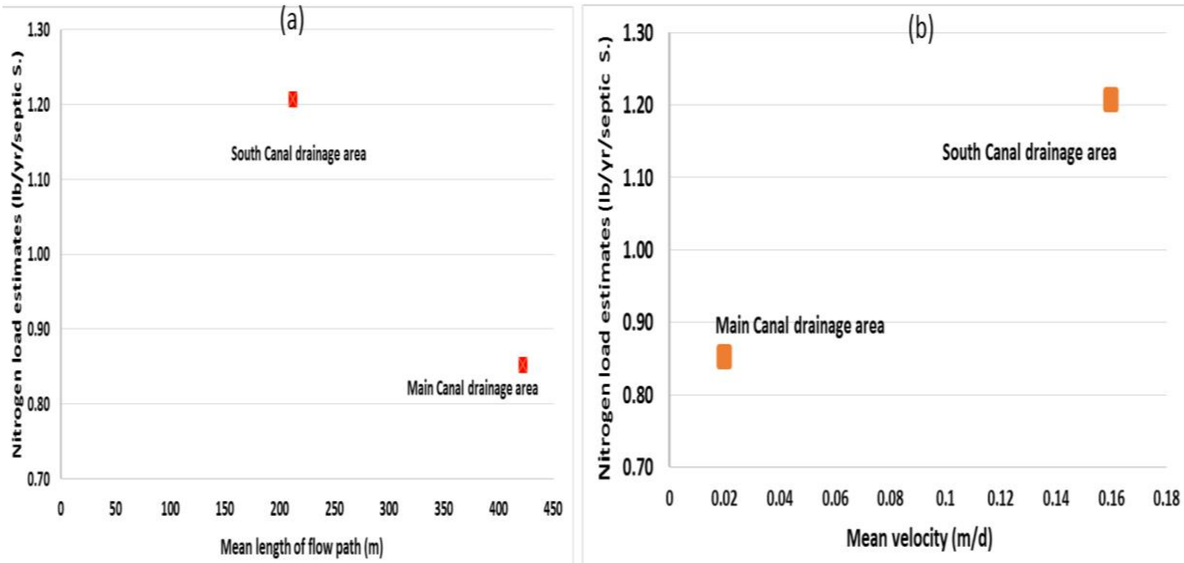

Figure 4-8. Variation of nitrogen load estimate per septic systems with (a) mean length of flow path (m), and (b) mean velocity (m/d), in the main and south canal drainage basin area.

Figure 4-23 plots the load estimate and soil drainage conditions in the Port St. Lucie site. Figure 4-24 does the same for a total of five sites, excluding Banner Lake and Hobe Sound sites where there is only one drainage category (excessively drainage). The drainage conditions are classified in the SSURGO database into seven categories: excessively drained (ED), somewhat excessively drained (SED), well drained (WD), moderately well drained (MWD), somewhat poorly drained (SPD), poorly drained (PD), and very poorly drained (VPD). For each drainage category, the number of septic systems is counted and the load from the septic systems is calculated, which is used for plotting Figures 4-23 and 4-24. Figure 4-23 shows that the load estimate increases when the drainage condition changes from very poorly drained to excessively drained. This is not surprising because nitrogen transport in faster well-drained soil is faster than in poorly drained soil. Figure 4-24(a) shows the groundwater velocity increases when the drainage condition changes from very poorly drained to excessively drained. However, the relation between the load estimates and soil drainage conditions is not observed in the other four sites plotted in Figures 4-24(b)-(e). A possible reason is that, at the four sites, the removed septic systems are located in areas smaller than that in the Port St. Lucie site. In addition, the numbers of removed septic systems are also smaller than those in the Port St. Lucie site. As a result, the relation at the four sites is less statistically meaningful than that at the Port St. Lucie site.

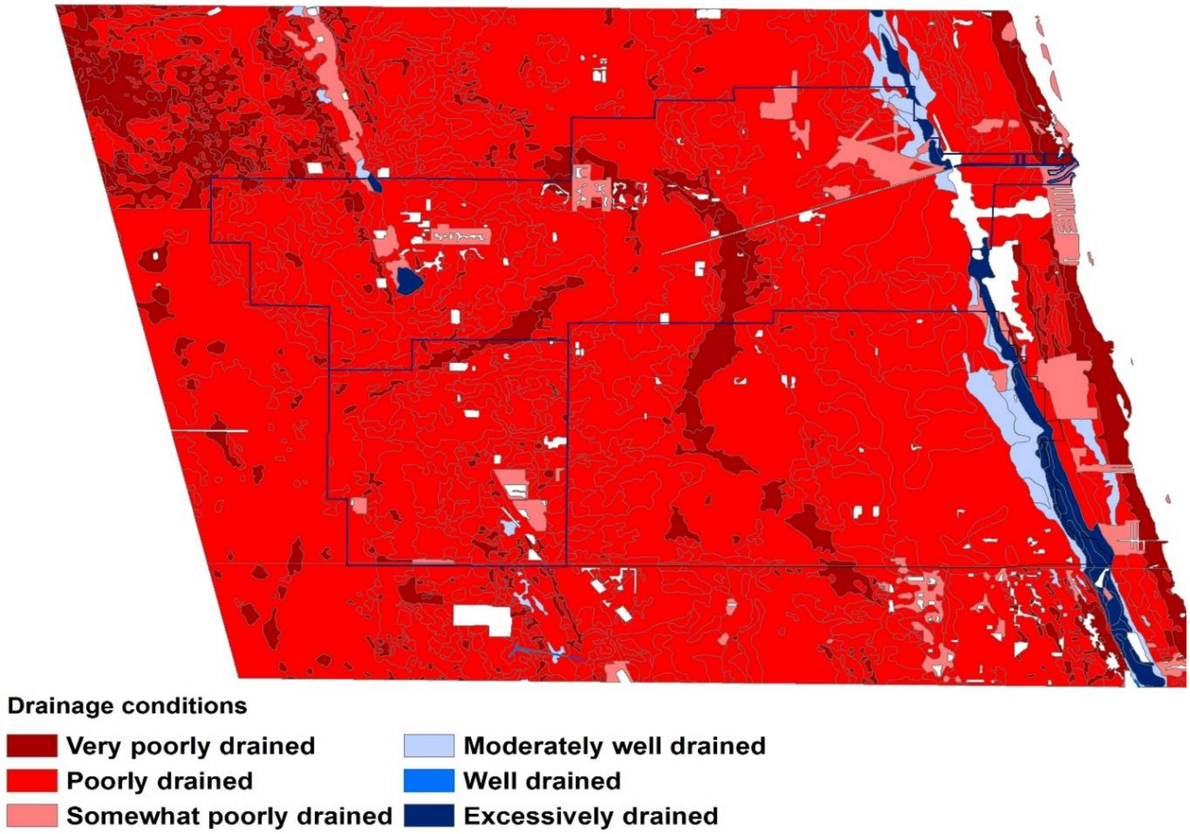

Figure 4-9. Variation of nitrogen load estimate per septic systems with drainage conditions of the soil zones where septic systems are located at the main-south canal drainage area.

5. Ammonium (NH4) and Nitrate-Nitrite (NOx) load estimation

This section is going to emphasize the results and the findings of the proportion of NH4 and NOx concentration using VZMOD, which is the input concentration for ArcNLET. First to apply the VZMOD; and generated septic tanks file was used for the ArcNLET to simulate the NH4 and NOx concentrations.

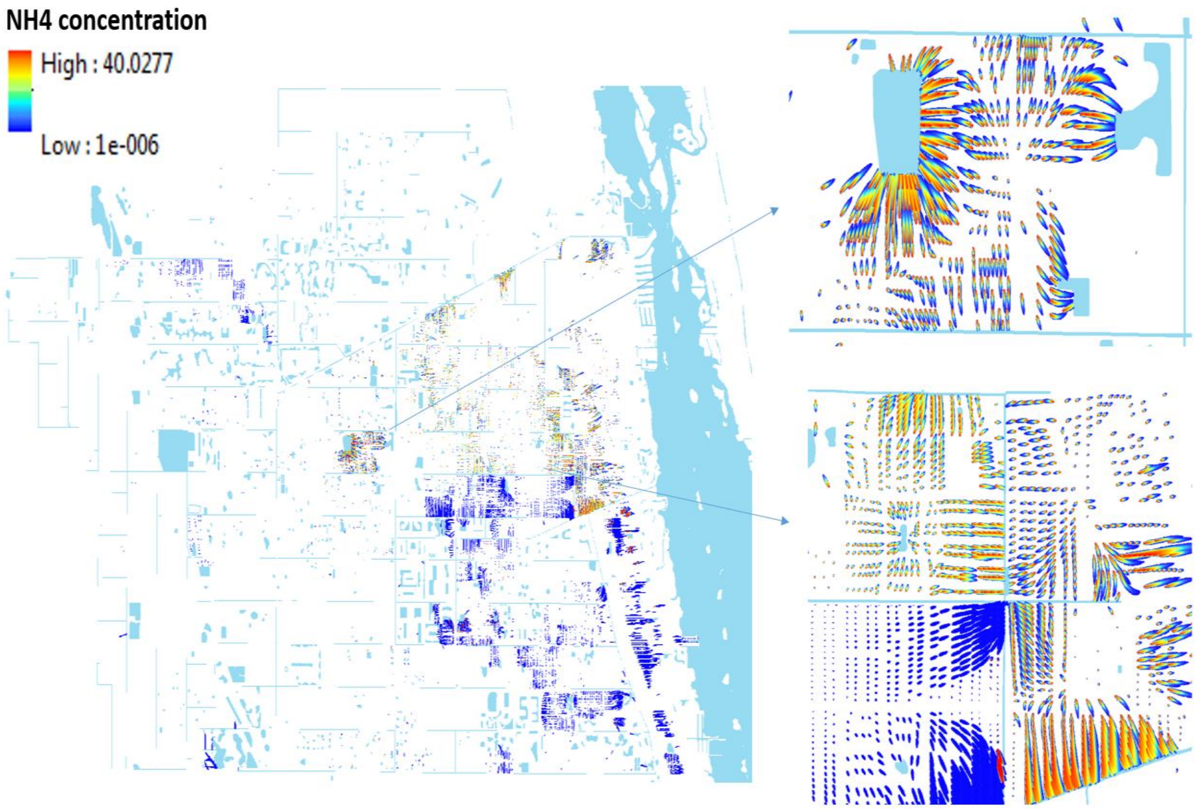

Figure 5-1. NH4 plume concentration and distribution.

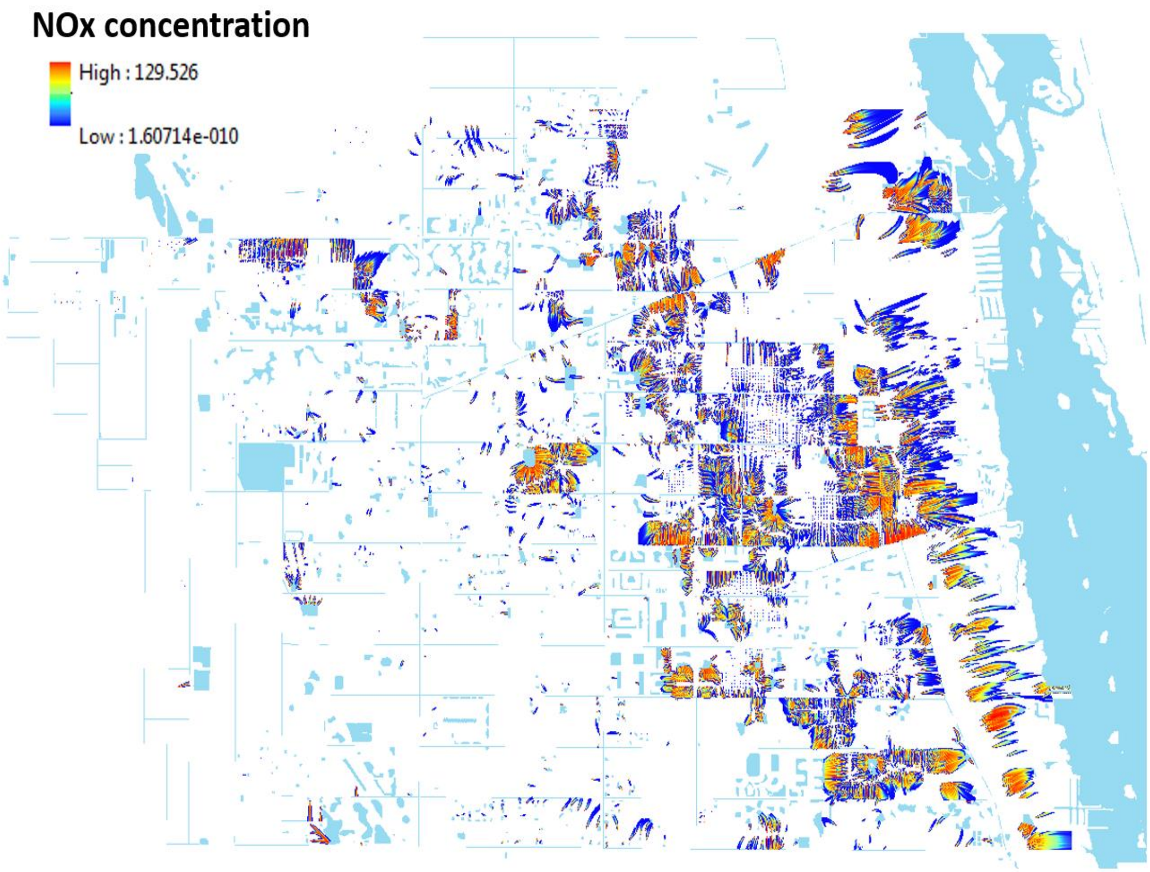

Figure 5-2. NOx plume concentration and distribution.

Table 5.1: Loading summary

	Total output Load (g/d)	**Total output Load (lbs/yr)**	Total Denitrification (g/d)	Total Input Mass (g/d)	Load Reduction (%)	**Load/Septic Tank (g/d)**	**Load/Septic Tank (lbs/yr)**
NH4	**93.73**	**75.44**	1909.40	2003.13	95.32	**0.01**	**0.01**
NO3	**17505.70**	**14089.03**	231467.42	248973.13	92.97	**1.37**	**1.11**
Total	**17599.43**	**14164.47**	233376.82	250976.25	92.99	**1.38**	**1.12**

Table 5.2: Transport and other parameters in new ArcNLET

Parameter	**IRL (SM canal of IRC)**
C_0 (mg/L)	VZMOD septic tank files
α_L (m)	1
α_{TH} (m)	0.1
K_{den} (d^{-1})	0.00055
K_{nit} (d^{-1})	0.00025
M_{in} (mg/d)	20966

6. CONCLUSIONS

This study uses ArcNLET to estimate nitrogen load from removed septic systems to surface water bodies in the Indian River Lagoon located within the South-Main Canal drainage basin in Indian River County. This study leads to the following major conclusions:

Data and information needed to establish ArcNLET models for nitrogen load estimation are readily available in the modeling areas. The data of DEM, surface water bodies, and hydraulic conductivity can be downloaded from public-domain databases. FDEP and environmental agencies of the cities and counties have site-specific data and information such as locations of canals and septic systems. Therefore, ArcNLET models can be set up easily for other areas of interest to support the on-going BMAP.

Although there is no recent groundwater monitoring network, historical data are used for calibration provided by the FDEP personnel. The data compiled in this study indicate that ammonium/TKN concentrations are significant and in general higher than NO_x concentrations in the study areas. However, the available data are limited and outdated. While the observations of water table may represent the groundwater flow system, nitrogen concentrations may not reflect the current system of nitrogen transport, which leads to limited understanding of nitrogen transport at the modeling sites. However recent data collection is undergoing, once the data will be available new modeling can be supersede the existing model owing to the new calibration.

REFERENCES

Anderson, D. (2006), A Review of Nitrogen Loading and Treatment Performance Recommendations for Onsite Wastewater Treatment Systems (OWTS) in the Wekiva Study Area, Hazen and Sawyer, P.C.

Aravena, R. and Robertson, W. D. (1998), Use of Multiple Isotope Tracers to Evaluate Denitrification in Ground Water: Study of Nitrate from a Large-Flux Septic System Plume. Ground Water, 36: 975–982. doi: 10.1111/j.1745-6584.1998.tb02104.x

Aziz, C.E., Newell, C.J., Gonzales, J.R., Haas, P., Clement, T.P., Sun, Y. (2000) BIOCHLOR natural attenuation decision support system user's manual version 1.0. U.S. Environmental Protection Agency, Washington, DC

Balci, P., L. Bertolotti, K. Carter, and C. Conrad (2012), Appendix 10-1: St. Lucie River Watershed Protection Plan Update. In: 2012 South Florida Environmental Report, Appendix 10-1. South Florida Water Management District (SFWMD), West Palm Beach, FL.

Beaujouan, V., P. Durand, L. Ruiz, P. Aurousseau, G. Cotteret (2002), A hydrological model dedicated to topography-based simulation of nitrogen transfer and transformation: rationale and application to the geomorphology-denitrification relationship. Hydrol Process 16(2):493–507.

Belanger, T.V., H.H. Heck, C. Gefvert, and S. Krupa (2004), Seepage meter program for St. Lucie River and Indian River Lagoon, South Florida Water Management District (SFWMD), Florida Institute of Technology, Melbourne, FL.

Belanger, T.V., T.L. Price, and H.H. Heck (2007), Submarine groundwater discharge in the Indian River Lagoon, Florida. How important is it? Hydrological Sciences, 4, 344-362.

Belanger, T.V., T.L. Price, and D.I. McGinnis (2009), The Importance of OSTDS Contaminant Loading to the IRL, Final Project Report for Contract 25141 of St. Johns River Water Management District, Melbourne, FL.

BMAP (2012), Basin Management Action Plan for the Implementation of Total Maximum Daily Loads for Nutrients and Dissolved Oxygen by the Florida Department of Environmental Protection in the Santa Fe River Basin, developed by the Florida Department of Environmental Protection Division of Environmental Assessment and Restoration Bureau of Watershed Restoration.

BMAP (2013), Basin Management Action Plan for the Implementation of Total Maximum Daily Loads for Nutrients and Dissolved Oxygen by the Florida Department of Environmental Protection in the St. Lucie River and Estuary Basin, Developed by the St. Lucie River and Estuary Basin Technical Stakeholders.

Bowen, J.L., J.M. Ramstack, S. Mazzilli, and I. Valiela (2007), NLOAD: an interactive, web-based modeling tool for nitrogen management in estuaries. Ecological Applications, 17, S17–S30.

Collins, G., J.N. Kremer, and I. Valiela (2000), Assessing uncertainty in estimates of nitrogen loading to estuaries for research, planning, and risk assessment, Environmental Management, 25(6), 635-645, DOI: 10.1007/s002670010050.

Delgado J.M.P.Q., (2007), Longitudinal and Transverse Dispersion in Porous Media, Chemical Engineering Research and Design, 85(9): 1245-1252.

Domenico, P.A. (1987) An analytical model for multidimensional transport of a decaying contaminant species. J Hydrol 91:49–58.

Dann K. Yobbi. (1996), Simulation of Subsurface Storage and Recovery of Treated Effluent Injected in a Saline Aquifer, St. Petersburg, Florida. U.S. GEOLOGICAL SURVEY, Water-Resources investigations report 95-4271.

Gelhar, L.W., C. Welty, and K.R. Rehfeldt. (1992), A critical review of data on field-scale dispersion in aquifers. Water Resour. Res. 28: 1955–1974.

Giordano, J.C.P., M. J. Brush, and I.C. Anderson (2011), Quantifying annual nitrogen loads to Virginia's coastal lagoons: sources and water quality response, Estuaries and Coasts, 34, 297–309, DOI 10.1007/s12237-010-9345-7.

Fernandes, R. (2011), Statistical methods for estimating the denitrification rate. Florida State University, Master Thesis.

Hanisak, M.D., (2002), Benthic Nutrient Flux in St. Lucie Estuary, A data report prepared as part of a cooperative agreement with South Florida Water Management District.

Harden, H., J. Chanton, R. Hicks, and E. Wade (2010), Wakulla County Septic Tank Study Phase II Report on Performance Based Treatment Systems.

Heinen, M (2006) Simplified denitrification models: Overview and properties. Geoderma 133(3-4):444–463

Helsel, D.R. and R. M. Hirsch, 2002. Statistical Methods in Water Resources Techniques of Water Resources Investigations, Book 4, chapter A3. U.S. Geological Survey. 522 pages.

Herr, J., L. Weintraub, C.W. Chen (2001), User's Guide to WARMF, Documentation of Graphical User Interface.

Howarth, R.W., D. Anderson, J. Cloern, C. Elfring, C. Hopkinson, B. Lapointe, T. Malone, N. Marcus, K. McGlathery, A. Sharpley, and D. Walker (2000), Nutrient pollution of coastal rivers, bays, and seas. Issues in Ecology, 7, 1-15.

Howath, R.W. (2008), Coastal nitrogen pollution: A review of sources and trends globally and regionally, Harmful Algea, 8, 14-20.

Jahangir, M.M.R, Johnston, P., Khalil, M.I., et al. Linking hydrogeochemistry to nitrate abundance in groundwater in agricultural settings in Ireland. Journal of Hydrology, 2012, 212-222.

Kaufman, G. J.L. Oliver, D.A. Thomas, T. Woolm L.L. Yuan, J. Butcher, J. Gerritsen, M.J. Paul, and L. Zheng (2010), Technical Support Document for U.S. EPA's Final Rule for Numeric Criteria for Nitrogen/Phosphorus Pollution in Florida's Inland Surface Fresh Waters. http://water.epa.gov/lawsregs/rulesregs/upload/floridatsd1.pdf

Kinney, E.L. and I. Valiela (2011), Nitrogen loading to Great South Bay: land use, sources, retention, and transport from land to bay, Journal of Coastal Research, 27(4), 672-686.

Kroeger, K.D., M.L. Cole, J.K. York, and I. Valiela (2006), Nitrogen Loads to Estuaries from Waste Water Plumes: Modeling and Isotopic Approaches, Ground Water, 44(2), 188-200.

Lapointe, B.E., L. W. Herren, and B. J. Bedford (2012), Effects of Hurricanes, Land Use, and Water Management on Nutrient and Microbial Pollution: St. Lucie Estuary, Southeast Florida, Journal of Coastal Research, 28(6), 1345–1361.

Lichtler, W. F. 1960. Geology and Groundwater Resources of Martin County, Florida.

Florida Geological Survey: Report of investigations: 23, 149p.

Lin YF, Wang JH, Valocchi AJ (2009) PRO-GRADE: GIS toolkits for groundwater recharge and discharge estimation. Ground Water 47(1): 122-128.

MACTEC, (2007). Phase I Report Wekiva River Basin Nitrate Sourcing Study. Newberry, FL: MACTEC http://www.dep.state.fl.us/water/wekiva/docs/phase-i-final-report.pdf

Maggi, F., C. Gu, W.J. Riley, G.M. Hornberger, R.T. Venterea, T. Xu, N. Spycher, C. Steefel, N.L. Miller, C.M. Oldenburg (2008), A mechanistic treatment of the dominant soil nitrogen cycling processes: Model development, testing, and application. J Geophys Res. doi:10.1029/2007JG000578.

Maizel, M.S., G. Muehlbach, P. Baynham, J. Zoerker, D. Monds, T. Iivari, P. Welle, J. Robbin, and J. Wiles (1997), The potential for nutrient loadings from septic systems to ground and surface water resources and the Chesapeake Bay. U.S. Environmental Protection Agency #903-R–97–006 Report No. CBP/TRS 166/97.

McCray, J.E., M. Geza, K.F. Murray, E.P Poeter, D. Morgan (2009), Modeling onsite wastewater systems at the watershed scale: a user's guide. Water Environment Research Foundation, Alexandria, VA.

McCray, JE, Kirkland SL, Siegrist RL, Thyne GD (2005) Model parameters for simulating fate and transport of on-site wastewater nutrients. Ground Water 43(4):628–639.

Meile, C., W.P. Porubsky, R.L. Walker, and K. Payne (2010), Natural attenuation of nitrogen loading from septic effluents: Spatial and environmental controls, Water Research, 4 4, 1399 – 1408.

Merrit, M.L., (1996), Numerical simulation of a plume of brackish water in the Biscayne aquifer originating from a flowing artesian well, Dade County, Florida: U.S. Geological Survey Water-Supply Paper 2462, 74 p.

Miller, W. L. 1979. Hydrologic and Geologic Data from the Upper East Coast Planning Area, Southeast Florida. USGS Open File Report 79 – 1543. Tallahassee, FL.

National Research Council (2000), Clean Coastal Waters: Understanding and Reducing the Effects of Nutrient Pollution. National Academies Press, Washington, DC.

National Research Council (2010) Understanding the Changing Planet Strategic Directions for the Geographical Sciences. Washington, D.C., National Academies Press.

Newell CJ, McLeod KR, Gonzales JR (1996) BIOSCREEN, natural attenuation decision support system, user's manual, version 1.3. EPA/600/R-96-087. U.S. Environmental Protection Agency, Washington, DC

Porubsky, W.P., S.B. Joye, W.S. Moore, K. Tuncay, C. Meile (2011), Field measurements and modeling of groundwater flow and biogeochemistry at Moses Hammock, a backbarrier island on the Georgia coast, Biogeochemistry, 104 (1-3), 69-90, DOI: 10.1007/s10533-010-9484-8.

Reay, W.G. (2004), Septic tank impacts on ground water quality and nearshore sediment nutrient flux, Ground Water, 42(7), 1079-1089.

Rehfeldt, K. R., and L. W. Gelhar, (1992), Stochastic analysis of dispersion in unsteady flow in heterogeneous aquifers, Water Resour. Res., 28(8), 2085–2099, doi:10.1029/92WR00750.

Rios, J.F. (2010), A GIS-Based Model for Estimating Nitrate Fate and Transport from Septic Systems in Surfacial Aquifers, Master Thesis, Florida State University, Tallahassee, FL.

Rios, J.F., M. Ye, and L. Wang (2011a), uWATER-PA: Ubiquitous WebGIS Analysis Toolkit for Extensive Resources - Pumping Assessment, Ground Water, 49(6), 776-780, DOI: 10.1111/j.1745-6584.2011.00872.x.

Rios, J.F., M. Ye, L. Wang, and P. Lee (2011b), ArcNLET: An ArcGIS-Based Nitrate Load Estimation Toolkit, User's Manual, Florida State University, Tallahassee, FL., available online at http://people.sc.fsu.edu/~mye/ArcNLET/users_manual.pdf.

Rios, J.F., M. Ye, L. Wang, P.Z. Lee, H. Davis, and R.W. Hicks (2013a), ArcNLET: A GIS-based software to simulate groundwater nitrate load from septic systems to surface water bodies, Computers and Geosciences, 52, 108-116, 10.1016/j.cageo.2012.10.003.

Rios, J.F., M. Ye, and H. Sun (2013b), ArcNLET 2.0: New ArcNLET Function of Monte Carlo Simulation for Uncertainty Quantification, Florida State University, Tallahassee, FL.

Robertson, W.D., J.A. Cherry, and E.A. Sudicky (1991), Ground-Water Contamination from Two Small Septic Systems on Sand Aquifers. Ground Water, 29: 82–92. doi: 10.1111/j.1745-6584.1991.tb00500.x

Robertson, W. D. and J. A. Cherry (1992). Hydrogeology Of An Unconfined Sand Aquifer And Its Effect On The Behavior Of Nitrogen From A Large-Flux Septic System. Applied Hydrogeology 0(0): 32-44.

Roeder, E. (2008), Revised Estimates of Nitrogen Inputs and Nitrogen Loads in the Wekiva Study Area. Available online at http://www.dep.state.fl.us/water/wekiva/docs/doh-wekiva-estimate-final2008.pdf.

Romshoo, S.A. and M. Muslin (2011), Geospatial modeling for assessing the nutrient load of a Himalayan lake. Environ Earth Sci. doi:10.1007/s12665-011-0944-9.

Shirmohammadi, A., I. Chaubey, R.D. Harmel, D.D. Bosch, R. Muñoz-Carpena, C. Dharmasri, A. Sexton, M. Arabi, M.L. Wolfe, J. Frankenberger, C. Graff, T.M. Sohrabi (2006), uncertainty in TMDL models, Transactions of the ASABE, 49 (4): 1033-1049.

Sigua, G.C., Steward, J.S., Tweedale, W.A. (2000), Water quality monitoring and biological integrity assessment in the Indian River Lagoon, Florida: status, trends, and loadings (1988–1994). J. Environ. Manage. 25 (2), 199–209.

Sigua, G.C. and W.A. Tweedale (2003), Watershed scale assessment of nitrogen and phosphorus loadings in the Indian River Lagoon basin, Florida, Journal of Environmental Management, 67, 363–372.

Smith, C.G., Cable, J.E., Martin, J.B., Roy, M. (2008), Evaluating the source and seasonality of submarine groundwater discharge using a radon-222 pore water transport model. Earth and Planetary Science Letters, 273, pp. 312–322

Soil and Water Engineering Technology (SWET), (2008). Preliminary Report (DRAFT) for Project Entitled Nutrient Loading Rates, Reduction Factors and Implementation Costs Associated with BMPs and Technologies.

South Florida Water Management District (SFWMD), (2012). P.Balci, L. Bertolotti, K. Carter, and C. Conrad. Appendix 10-1: St. Lucie River Watershed Protection Plan Update. In: 2012 South Florida Environmental Report, Appendix 10-1.

Spiteri, C., C. P. Slomp, K. Tuncay, and C. Meile (2008), Modeling biogeochemical processes in subterranean estuaries: Effect of flow dynamics and redox conditions on submarine groundwater discharge of nutrients, Water Resour. Res., 44, W02430, doi:10.1029/2007WR006071.

Srinivasan V, Clement TP, Lee KK (2007) Domenico solution – is it valid? Ground Water 45(2):136–146.

Tesoriero, A. J., and L. J. Puckett (2011), O_2 reduction and denitrification rates in shallow aquifers, Water Resour. Res., 47, W12522, doi:10.1029/2011WR010471.

Toth, D.J. (1987), Hydrogology: Indian River Lagoon Joint Reconnaissance Report. St. Johns River Water Management District and South Florida Water Management District. Contract No. CM-137.

Thomas Obreza, Mark Clark, Brian Boman, et al. A Guide to EPA's Numeric Nutrient Water Quality Criteria for Florida. http://edis.ifas.ufl.edu/ss528

Ursin, E.L. and E. Roeder (2008), An assessment of nitrogen contribution from onsite wastewater treatment systems (OWTS) in the Wekiva study area of central Florida. In National Onsite Wastewater Recycling Association (NOWRA) Nitrogen Symposium. Florida Department of Health, Tallahassee.

U.S. EPA (2003), Voluntary National Guidelines for Management of Onsite and Clustered (Decentralized) Wastewater Treatment Systems. U.S. Environmental Protection Agency.

U.S. EPA. (2010), Water Quality Standards for the State of Florida’s Lakes and Flowing Waters; Proposed Rule. Released by EPA on January 14, 2010. http://edocket.access.gpo.gov/2010/pdf/2010-1220.pdf

U.S. EPA (2013), A Model Program for Onsite Management in the Chesapeake Bay Watershed, Office of Wastewater Management, U.S. Environmental Protection Agency.

Vadeboncoeur, M.A., S.P. Hamburg, and D. Pryor (2010), Modeled nitrogen loading to narragansett bay: 1850 to 2015, Estuaries and Coasts, 33, 1113–1127, DOI 10.1007/s12237-010-9320-3.

Valiela, I. and J.E. Costa (1988), Eutrophication of Buttermilk Bay, a Cape Cod coastal embayment: Concentrations of nutrients and watershed nutrient budgets. Environmental Management 12, no. 4: 539–553.

Valiela, I., G. Collins, J. Kremer, K. Lajtha, M. Geist, B. Seely, J. Brawley, C.H. Sham (1997) Nitrogen loading from coastal watersheds to receiving estuaries: new method and application, Ecological Applications, 7(2), 358–380.

Valiela, I., M. Geist, J. McClelland, and G. Tomasky (2000), Nitrogen loading from watersheds to estuaries: Verification of the Waquoit Bay Nitrogen Loading Model. Biogeochemistry 49, no. 3: 277–293.

Walters, A.H. (1983), Nitrate controversy and cancer causation: an environmental viewpoint. Environmentalist 3:219–226. doi:10.1007/BF02240112.

Wang, L., M. Ye, J.F. Rios, and P. Lee (2011), ArcNLET: An ArcGIS-Based Nitrate Load Estimation Toolkit, Application Manual, Florida State University, Tallahassee, FL., available online at http://people.sc.fsu.edu/~mye/ArcNLET/application_manual.pdf.

Wang L, Ye M, J.F. Rios, Lee P (2012). Sensitivity analysis and uncertainty assessment for ArcNLET-estimated nitrate load from septic systems to surface water bodies. http://people.sc.fsu.edu/~mye/ArcNLET/ArcNLETSensitivityUncertainty.pdf

Wang, L., M. Ye, J.F. Rios, R. Fernandes, P.Z. Lee, and R.W. Hicks (2013), Estimation of nitrate load from septic systems to surface water bodies using an ArcGIS-based software, Environmental Earth Sciences, doi:10.1007/s12665-013-2283-5.

West, MR, Kueper, BH, Ungs, MJ (2007) On the use and error of approximation in the Domenico (1987) solution. Ground Water 45(2): 126–135.

Yang, YCE, Lin, YFF (2011) A new GIScience application for visualized natural resources management and decision support. Trans. In GIS 15(s1): 109-124